ORNL/NUREG/TM-175

Quarterly Progress Report on Blowdown Heat Transfer Separate-Effects Program for October–December 1977

D. G. Thomas
W. E. Baucum
R. E. Bohanan
R. C. Hagar
R. A. Hedrick
P. A. Jallouk
A. F. Johnson
L. J. Ott
A. N. Smith
K. G. Turnage
J. D. White

Prepared for the U.S. Nuclear Regulatory Commission
Office of Nuclear Regulatory Research
Under Interagency Agreements DOE 40-551-75 and 40-552-75

OAK RIDGE NATIONAL LABORATORY
OPERATED BY UNION CARBIDE CORPORATION · FOR THE DEPARTMENT OF ENERGY

Printed in the United States of America. Available from
National Technical Information Service
U.S. Department of Commerce
5285 Port Royal Road, Springfield, Virginia 22161
Price: Printed Copy $6.00; Microfiche $3.00

ORNL/NUREG/TM-175
Dist. Category NRC-2

Contract No. W-7405-eng-26

Engineering Technology Division

QUARTERLY PROGRESS REPORT ON BLOWDOWN HEAT TRANSFER SEPARATE-EFFECTS PROGRAM FOR OCTOBER—DECEMBER 1977

D. G. Thomas

W. E. Baucum	A. F. Johnson
R. E. Bohanan	L. J. Ott
R. C. Hagar	A. N. Smith
R. A. Hedrick	K. G. Turnage
P. A. Jallouk	J. D. White

Manuscript Completed — April 3, 1978
Date Published —April 1978

NOTICE: This document contains information of a preliminary nature. It is subject to revision or correction and therefore does not represent a final report.

Prepared for the
U. S. Nuclear Regulatory Commission
Office of Nuclear Regulatory Research
Under Interagency Agreements DOE 40-551-75 and 40-552-75

Prepared by the
OAK RIDGE NATIONAL LABORATORY
Oak Ridge, Tennessee 37830
operated by
UNION CARBIDE CORPORATION
for the
DEPARTMENT OF ENERGY

CONTENTS

PREVIOUS REPORTS IN THIS SERIES

Report No.	Period covered
ORNL/TM-4655 (Vol. 1)	April—June 1974
ORNL/TM-4729 (Vol. 1)	July—September 1974
ORNL/TM-4805 (Vol. 1)	October—December 1974
ORNL/TM-4914 (Vol. 1)	January—March 1975
ORNL/TM-5021 (Vol. 1)	April—June 1975
ORNL/TM-5117	July—September 1975
ORNL/TM-5240	October—December 1975
ORNL/NUREG/TM-14	January—March 1976
ORNL/NUREG/TM-46	April—June 1976
ORNL/NUREG/TM-61	July—September 1976
ORNL/NUREG/TM-92	October—December 1976
ORNL/NUREG/TM-109	January—March 1977
ORNL/NUREG/TM-134	April—June 1977
ORNL/NUREG/TM-149	July—September 1977

KEYWORDS

Pressurized-water reactor, blowdown heat transfer, separate effects, loss-of-coolant accident, Thermal-Hydraulic Test Facility (THTF), Forced Convection Test Facility (FCTF), electrical heater rods, bundle hydraulics, two-phase flow, COBRA IV, 49-rod bundle, pump seals, heater rod sheath thermocouples, test matrix, RELAP4, double-ended break, test 156, test 157, test 158, test 160, test 161, test 162, test 171, test 163, test 164R, test 165, liquid-level detector, Auburn meter, pump bearings, bundle 2 prototypes, instrument error analysis, dynamic response, heater failure, pump seal life, thermocouple failures, liquid-level measurement, turbine meter bearing life, heater rod diagnostics, THTF bundle 2, THTF bundle 3, inactive heater rod tests, heating element eccentricity, ORTCAL, PINSIM, surface heat flux perturbation, MgO-insulated thermocouples vs BN-insulated thermocouples.

QUARTERLY PROGRESS REPORT ON BLOWDOWN HEAT TRANSFER SEPARATE-EFFECTS PROGRAM FOR OCTOBER–DECEMBER 1977

D. G. Thomas

W. E. Baucum	A. F. Johnson
R. E. Bohanan	L. J. Ott
R. C. Hagar	A. N. Smith
R. A. Hedrick	K. G. Turnage
P. A. Jallouk	J. D. White

ABSTRACT

The Thermal-Hydraulic Test Facility (THTF) has completed 20 powered rod blowdowns through October 13, 1977. Of these blowdowns, 5 were completed with all 49 rods powered, 2 were completed with 2 inactive rods, and 13 were completed with 4 inactive rods. Initial system pressure was ∿15.5 MPa (∿2250 psi), test section inlet temperature was ∿559 K (∿547°F), and break area was equivalent to a 200% break with the total area usually split between inlet and outlet in the ratio 0.40:0.60. Heater rod power was 80, 100, or 122 kW/rod, and the test section temperature was ∿607 K (632°F), 598 K (617°F), or 589 K (600 °F). Mean time to critical heat flux (CHF) varied from 0.7 to 1.4 sec with delayed CHF of ∿2.5 sec occurring in the upper half of the bundle in some tests.

1. FORCED CONVECTION TEST FACILITY OPERATION

J. D. White P. H. Hayes

Bundle 2 heater rod 5N-11 has undergone three power drop tests and two blowdown tests in the Forced Convection Test Facility (FCTF). This heater rod is a sample taken from the lot of heaters purchased from Watlow Electric Company for Thermal-Hydraulic Test Facility (THTF) bundle 2 assembly. Three bundle 2 prototypical heaters have been tested previously in the FCTF with satisfactory results.[1-3] Heater 5N-11, however, is the first production line bundle 2 heater to be tested. Data from the power drop experiments have been supplied to the analysis group for calculations of contact coefficients and gap widths. Performance of the heater was satisfactory in all respects.

After the second blowdown experiment, the heater was removed from the FCTF so that a liquid-level device purchased from EG&G, Idaho National

Engineering Laboratory (INEL), might be tested in the FCTF. If the liquid-level probe survives the planned blowdown experiments in the FCTF, the probe will be used in the THTF bundle 2 for the measurement of liquid levels during THTF blowdown tests.

2. ANALYSIS

2.1 Data Management

R. M. Flanders
G. S. Massengill C. E. Davis
V. D. Clemons D. M. Leon

New engineering units codes for both the THTF and the FCTF are presently being debugged. The codes will use an instrument data base written on the raw data tapes to calculate engineering units, a technique which should eliminate the necessity for FORTRAN changes in the codes. The data reduction procedure for the THTF and FCTF is shown in Fig. 2.1.

2.2 Electric Pin Simulation

L. J. Ott
K. W. Childs* R. D. Dabbs
R. H. Greene M. D. White

ORTCAL (FCTF version 1, for dual-sheath heater designs) has been debugged and is operational. It has been used to analyze calibration data for bundle 2 prototypical heaters 5N-9 and 5N-13; coefficient data tapes have been prepared for all blowdowns in the FCTF involving these heaters. The FCTF version of ORTCAL, which is now debugged and operational, has also been adapted to evaluate single-sheath heaters.

ORINC (FCTF version 1, for dual-sheath heater designs) is operational and has been used to evaluate FCTF blowdown 77-1-3. Pending time step size and precision study results, the remainder of the FCTF blowdowns (for 5N-9 and 5N-13) will be evaluated. This version of ORINC has also been modified for single-sheath heater designs.

To study the possibility that heat-conduction limited situations may occur in the BDHT heaters during a blowdown, four codes (in various stages of development) are being generated to solve the parabolic formulation of the conduction equation. The techniques involved are

1. implicit solution of the inverse conduction problem,
2. explicit solution of the inverse conduction problem,

---

*Computer Sciences Division.

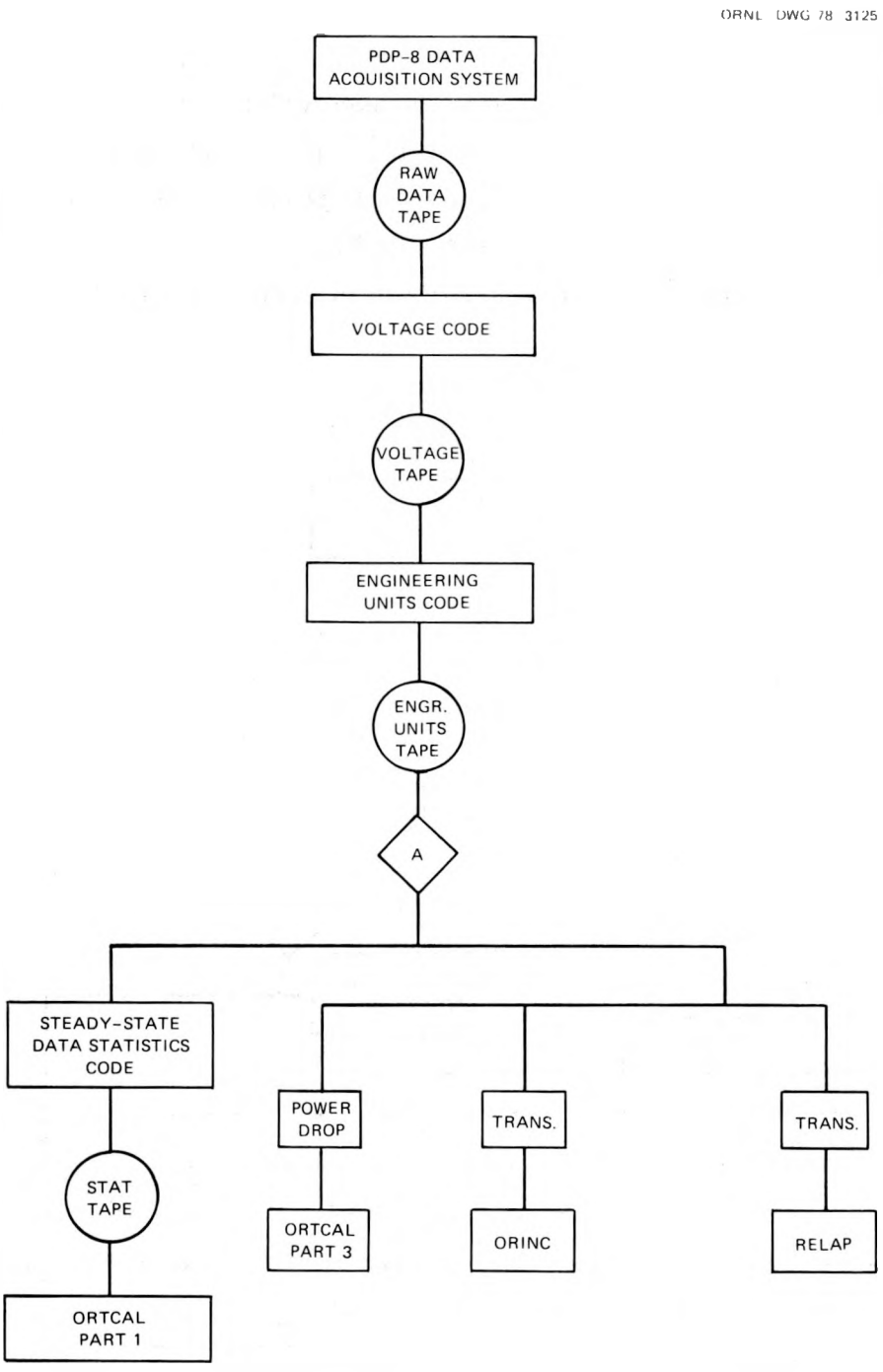

Fig. 2.1. Data reduction procedure for the THTF and FCTF.

3. implicit solution of the forward conduction problem,
4. explicit solution of the forward conduction problem.

Background work for the generation of a J. V. Beck type inverse code has been started. Several codes have been written to study interpolation order, time step size, loss of precision, and solution technique.

The interaction of the analysis task groups with respect to the pin simulation task group is illustrated in Figs. 2.2 and 2.3.

The documentation report on ORINC has been published.[4]

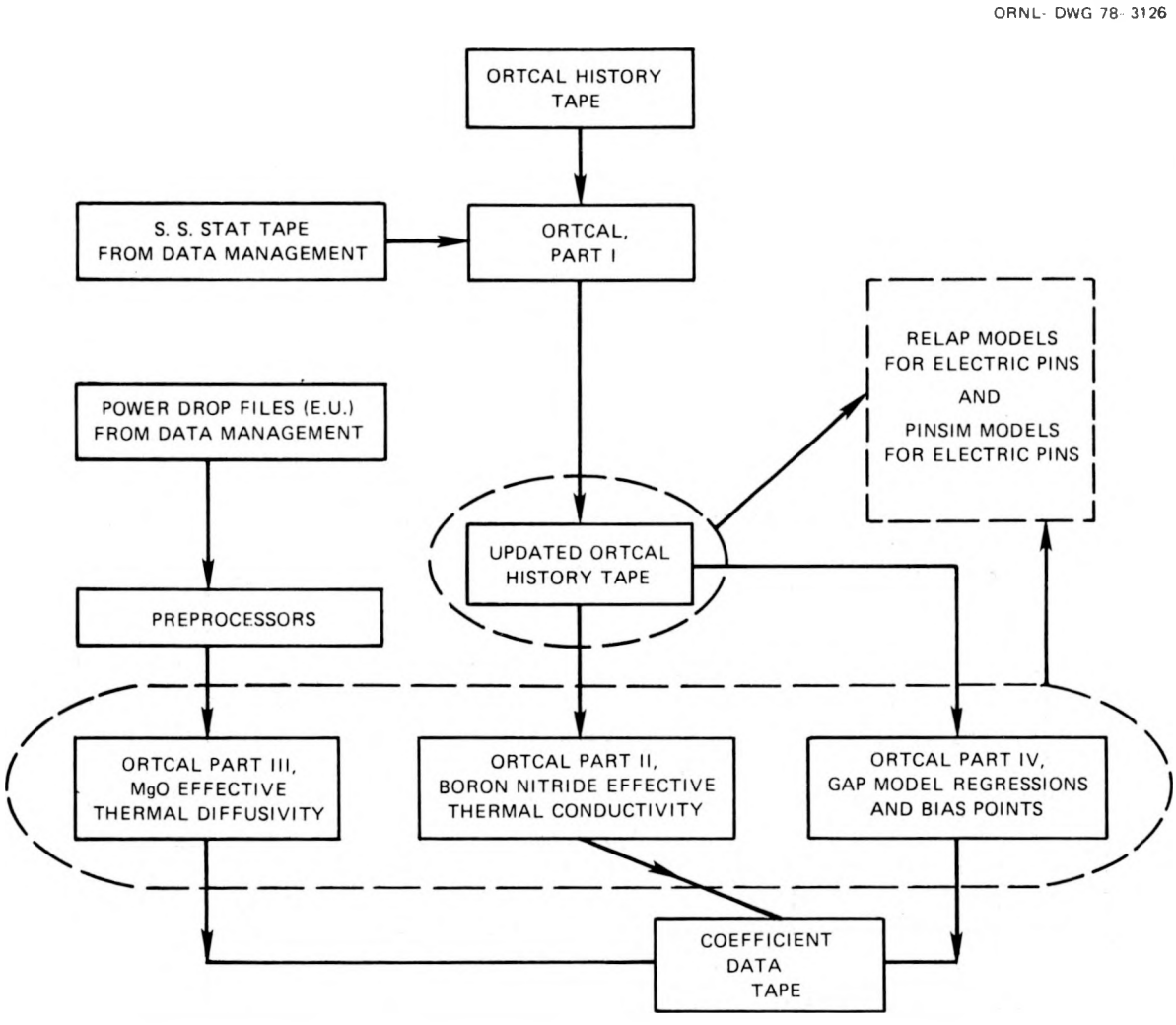

Fig. 2.2. Analysis task group interaction required for electric pin calibration.

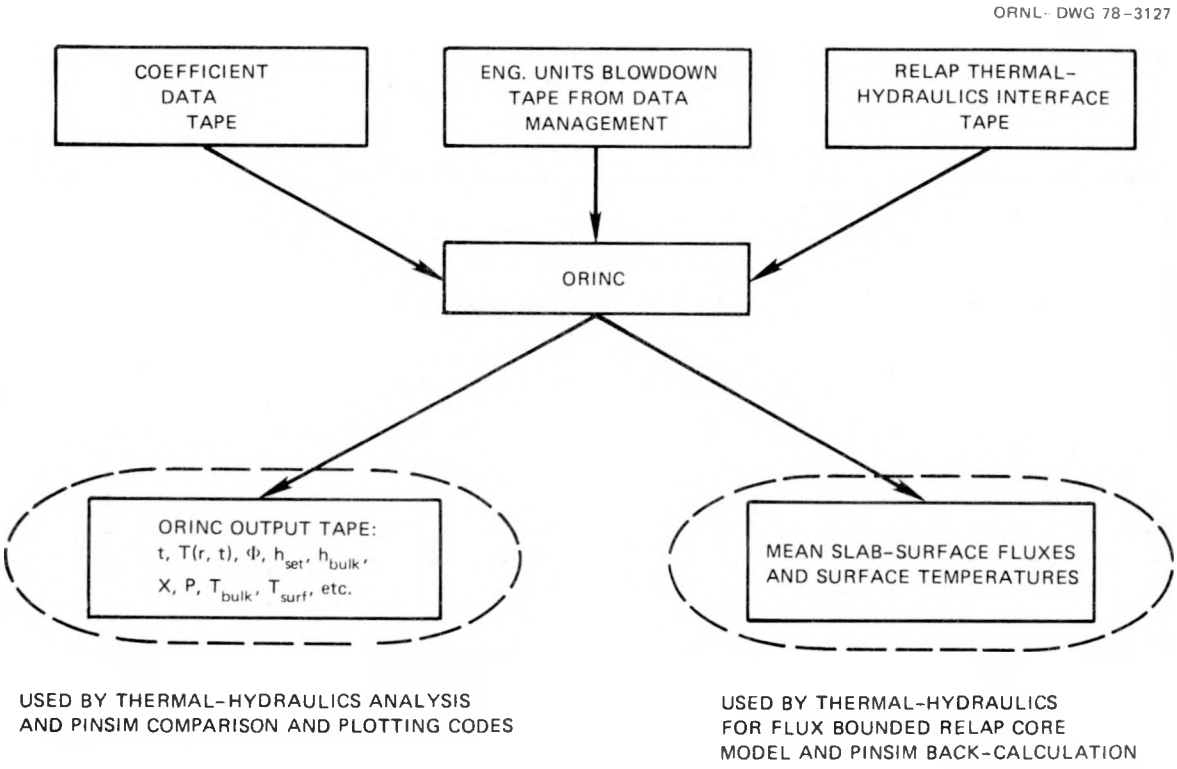

Fig. 2.3. Analysis task group interaction required for inverse calculations.

2.3 Nuclear Pin Simulation

R. C. Hagar G. M. Maxwell
J. L. Bartley E. D. Drennen*

Development of PINSIM-MOD 1 is nearing completion. Studies have indicated that the power back-calculation numerics are unstable at time step sizes smaller than approximately 50 msec. The code has been modified to time-average the back-calculation boundary conditions over smaller time steps until a suitable user-supplied period has elapsed.

The results of a PINSIM-MOD 1 electric pin power back-calculation are shown in Figs. 2.4 and 2.5. Figure 2.4 presents 6 sec of the RELAP4-MOD5—calculated nuclear fuel pin surface heat flux transient following a loss-of-coolant (LOCA) and the PINSIM-calculated transient electric pin

*Computer Sciences Division.

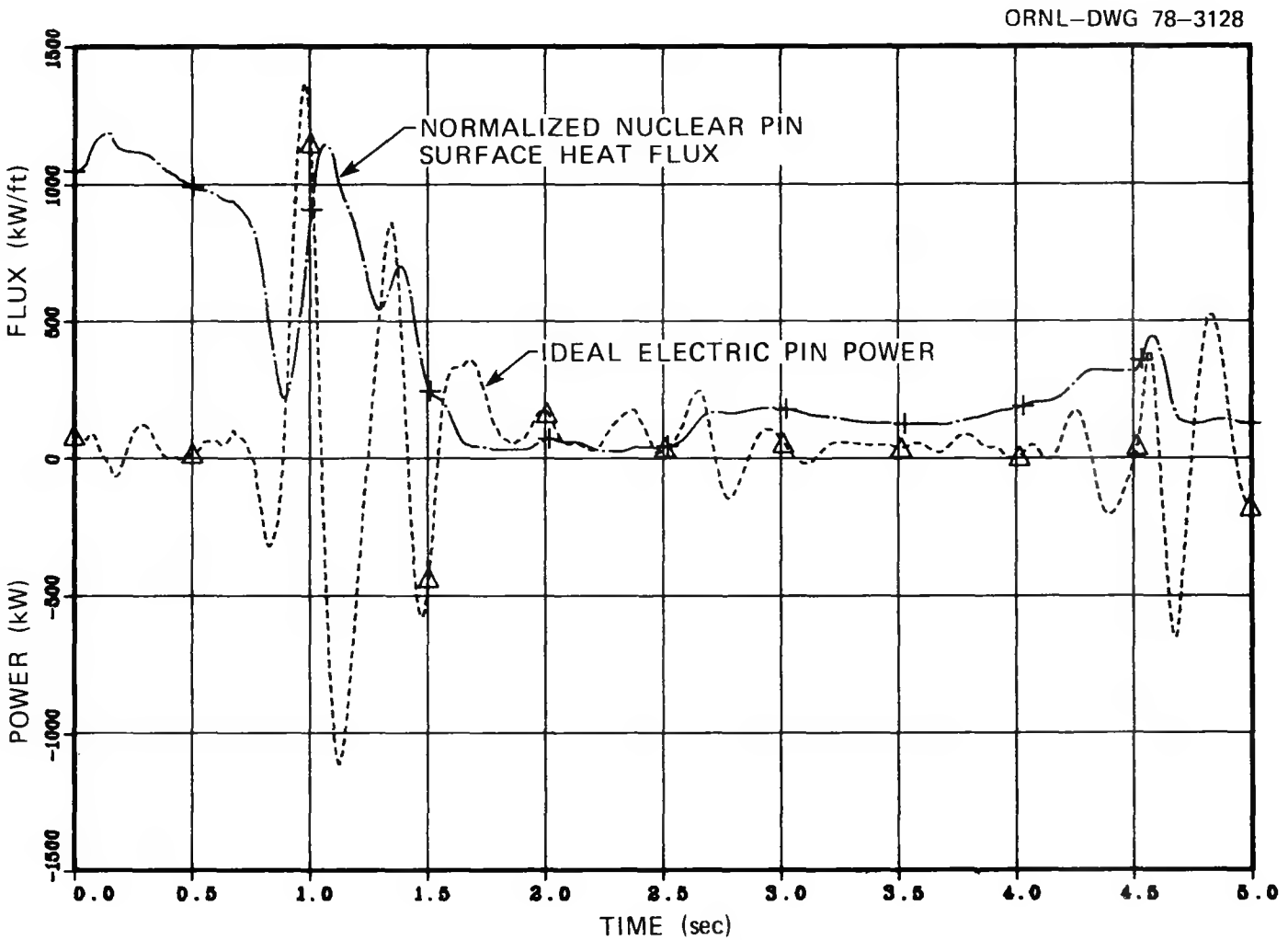

Fig. 2.4. Comparison of a normalized nuclear pin surface heat flux transient (calculated by RELAP4-MOD5) and the electric power (calculated by PINSIM) which must be supplied to a typical THTF electric pin to generate the same transient surface heat flux.

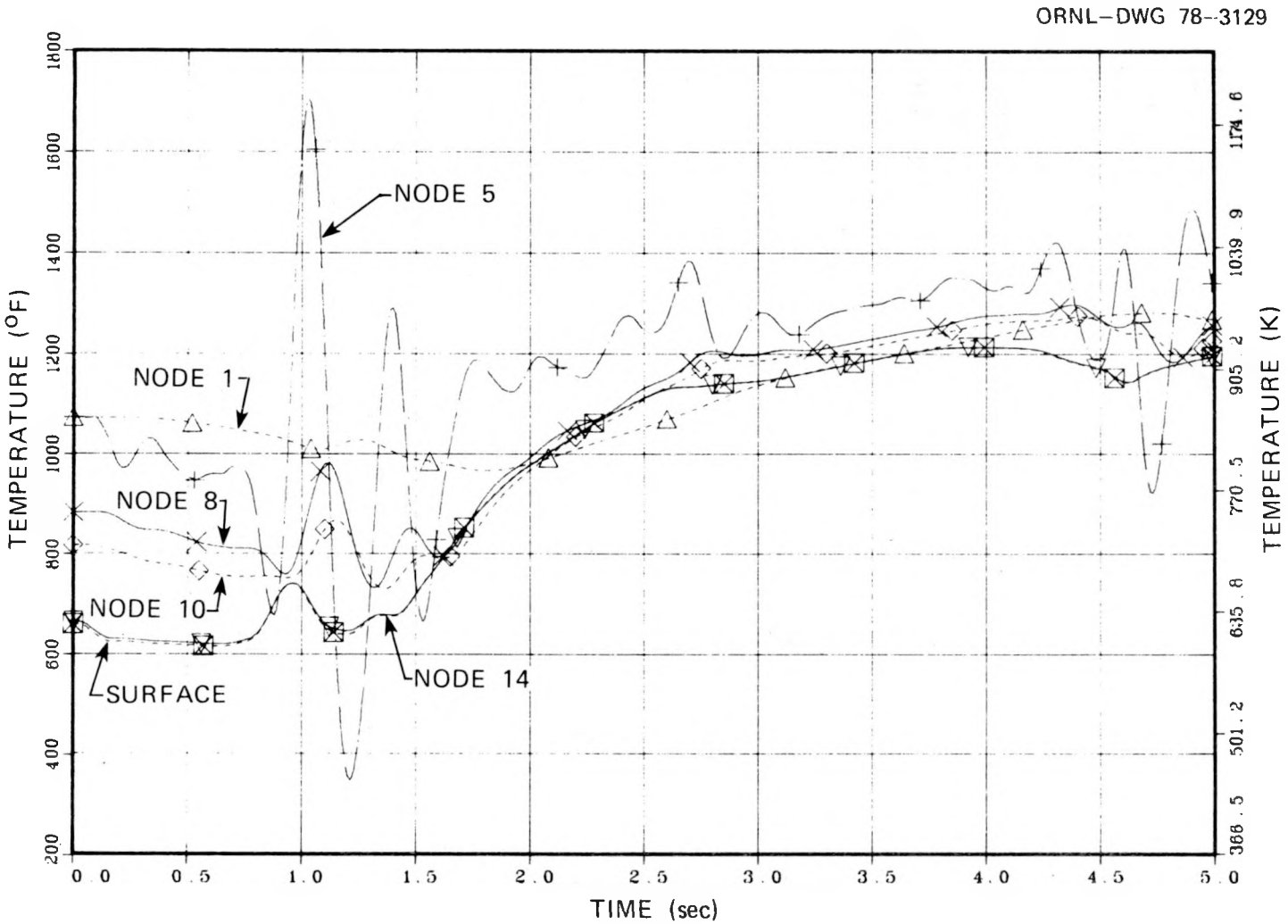

Fig. 2.5. Temperature histories of two internal nodes and of the surface of the electric pin model during the PINSIM calculation of the transient presented in Fig. 2.4.

power which must be supplied to a typical THTF bundle 1 pin simulator to generate the same surface heat flux response. (The surface heat flux values were time-averaged over 100 msec intervals for the back-calculation.) Figure 2.5 presents the PINSIM-calculated temperature histories of node 5, node 10, and the surface of the electric pin model. Node 5 corresponded to the heater element of the pin; the outermost node in the pin model was node 14.

Final debugging of the time-step-size selection algorithms is currently underway. (PINSIM-MOD1 is set up to determine suitable time step sizes within user-supplier limits or to accept user-supplied time step selections.) The algorithms used in PINSIM to calculate time step sizes are similar to those used in RELAP4-MOD5 and are designed to allow stable, accurate transient calculation to be performed in the shortest possible computer time.

Verification of PINSIM-MOD 1 is planned. Sample problems which will permit comparison of code results with both analytical problem solutions and those of established thermal-hydraulic codes are being prepared.

Preparation of PINSIM-MOD 1 documentation is underway. Included in the documentation will be presentation of the mathematical models and system modeling techniques used in the code, a description of the code structure and its major features, and a presentation and discussion of the results of several sample problem calculations.

Development of PINSIM-MOD 2 has begun. The major features which will distinguish MOD 2 from MOD 1 are the two-dimensional reactor kinetics module and the FRACAS-1 fuel-cladding deformation module. The two-dimensional kinetics module is intended to calculate transient axial power distributions in the nuclear pin models and is being adapted from the TWIGLE computer code; the adaptation is well underway. Copies of FRACAS-1 and MATPRO-6 have been obtained from INEL. Development of PINSIM-FRACAS interface subroutines has begun.

2.4 Thermal-Hydraulic Simulation

K. G. Turnage
W. G. Craddick C. R. Hyman
C. B. Mullins S. B. Cliff*

The radial variation in surface temperatures across the THTF heater rod bundle is being investigated. At a given axial level, four regions are defined, and as many as nine ORINC surface temperatures from each region are overlay plotted vs time during a blowdown. The temperature data band for each region is then characterized, and any radial effects are noted by comparing region to region.

Figures 2.6a and 2.6b show evidence of radial effects in rod surface temperatures calculated by the program ORINC. The plot designated "center" has the envelope of surface temperatures from rods farthest from the shroud box walls, and that designated "wall" has the envelope for those closest to the shroud box. The radial effect is not large and is not seen at all levels. Level E is just below the maximum power zone.

Three RELAP4 models of the THTF test section have been used to calculate surface temperature throughout the rod bundle for test 105. Single-, two-, and three-channel calculations were made using identical hydraulic boundary conditions at the test section inlet and outlet vertical spool pieces. The calculated radial variations in surface temperatures are being compared to variations actually observed in the rod bundle. The result should be an evaluation of the ability of the best estimate version of RELAP4 to predict radial effects in the THTF given presently available hydraulic boundary conditions and no cross-flow junctions. One of the three models may be chosen as the most practical for future use and development for calculating local fluid conditions in the THTF rod bundle during blowdowns.

Data comparisons of RELAP-predicted rod surface temperatures and those obtained from ORINC (based on sheath thermocouple response) have shown that agreement is better in the lower and middle parts of the THTF bundle. RELAP

---

*Computer Sciences Division.

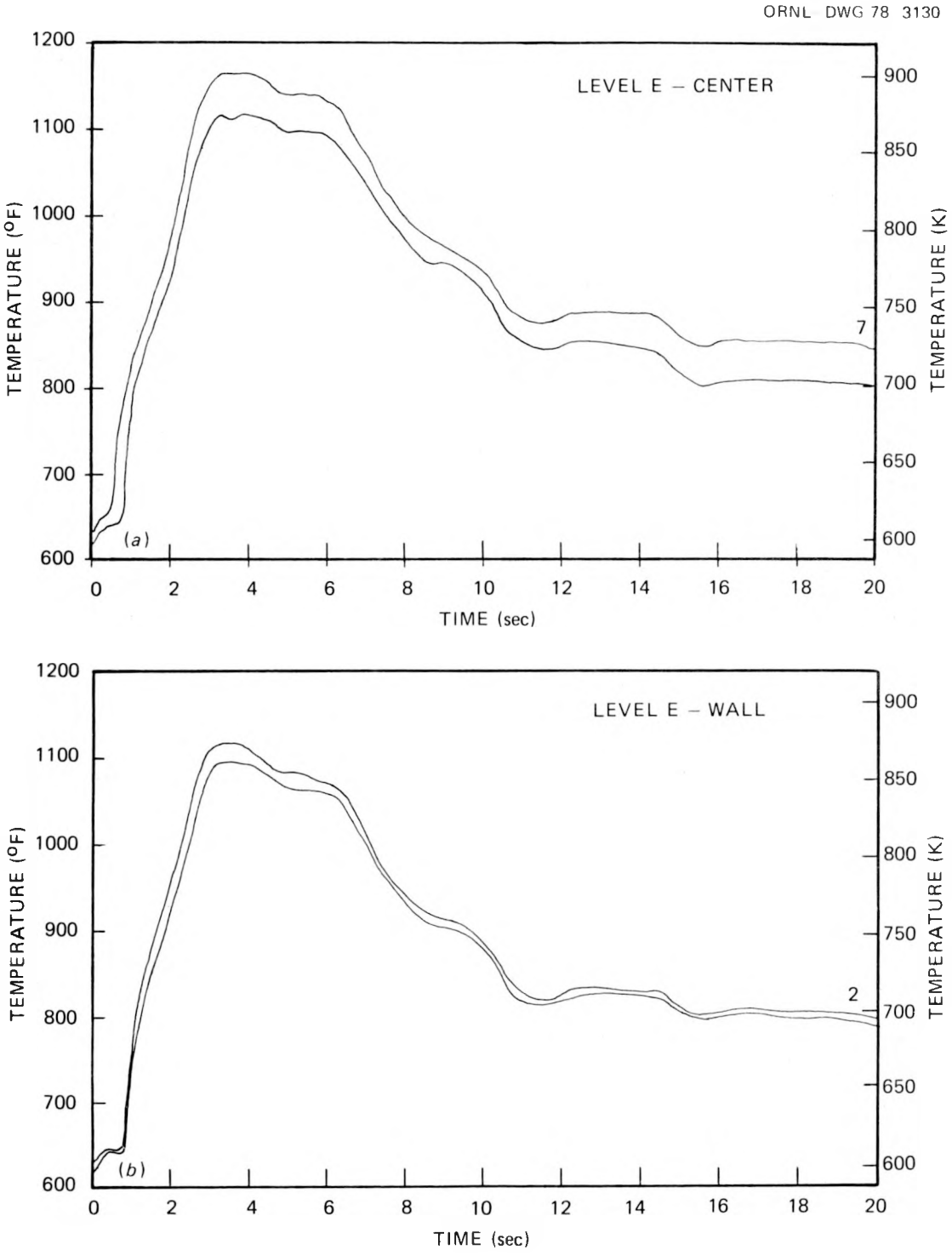

Fig. 2.6. Envelope of rod surface temperatures (ORINC) for rods farthest from the shroud box wall for level E (a). Envelope of rod surface temperatures (ORINC) for rods nearest the shroud box wall for level E (b).

tends to overpredict temperatures at thermocouple levels I and above (Fig. 2.7). Due to the lack of experimental fluid temperature and flow data within the rod bundle, it is difficult to define the problem as a result of RELAP code inadequacy, modeling errors, or poor hydraulic boundary conditions. In general, data available from fluid instrumentation in the THTF test section are being well predicted when experimental time-dependent boundary conditions are used. For example, see Fig. 2.8 which shows eight typical subchannel thermocouples (located just above the top of the bundle's heated zone) together with the fluid temperature predicted by a single-channel RELAP core model using experimental boundary conditions.

Checkout of a more detailed THTF system model for RELAP is proceeding. The model incorporates changes outlined in the Data Evaluation Report — System Response for Test Series 100. It will probably be used to provide hydraulic boundary conditions for a RELAP test section model in an evaluation of RELAP's ability to predict local fluid conditions in the THTF bundle independent of any boundary conditions from experimental data. The new system model has been run in steady state for 30 sec and in a blowdown calculation (test 105).

The RELAP fill table generator program is being updated. These changes make it possible to provide boundary conditions altered to reflect uncertainty in the instruments used to calculate mass flow and enthalpy. An arbitrary number of standard deviations in mass flux and/or enthalpy may be added to or subtracted from the best estimate value and the result used to drive a RELAP core model.

RLPSFLUX, a code produced at ORNL from the RELAP4/MOD5 source, has been used to simulate THTF tests 104 and 105. The code bypasses RELAP's heat transfer calculations and supplies best-estimate heat fluxes from ORINC for core sections where thermocouple data are available. Calculations with the heat flux boundary condition have been run to 7 sec on test 105 and 15 sec on test 104. Comparisons of fluid quality at the core midplane from the RLPSFLUX and RELAP4 calculations show good agreement (Fig. 2.9). When superheated steam is present, excessive fluid temperatures are sometimes calculated (Fig. 2.10). It should be possible to calculate transient heat transfer coefficients during some periods of blowdown at some

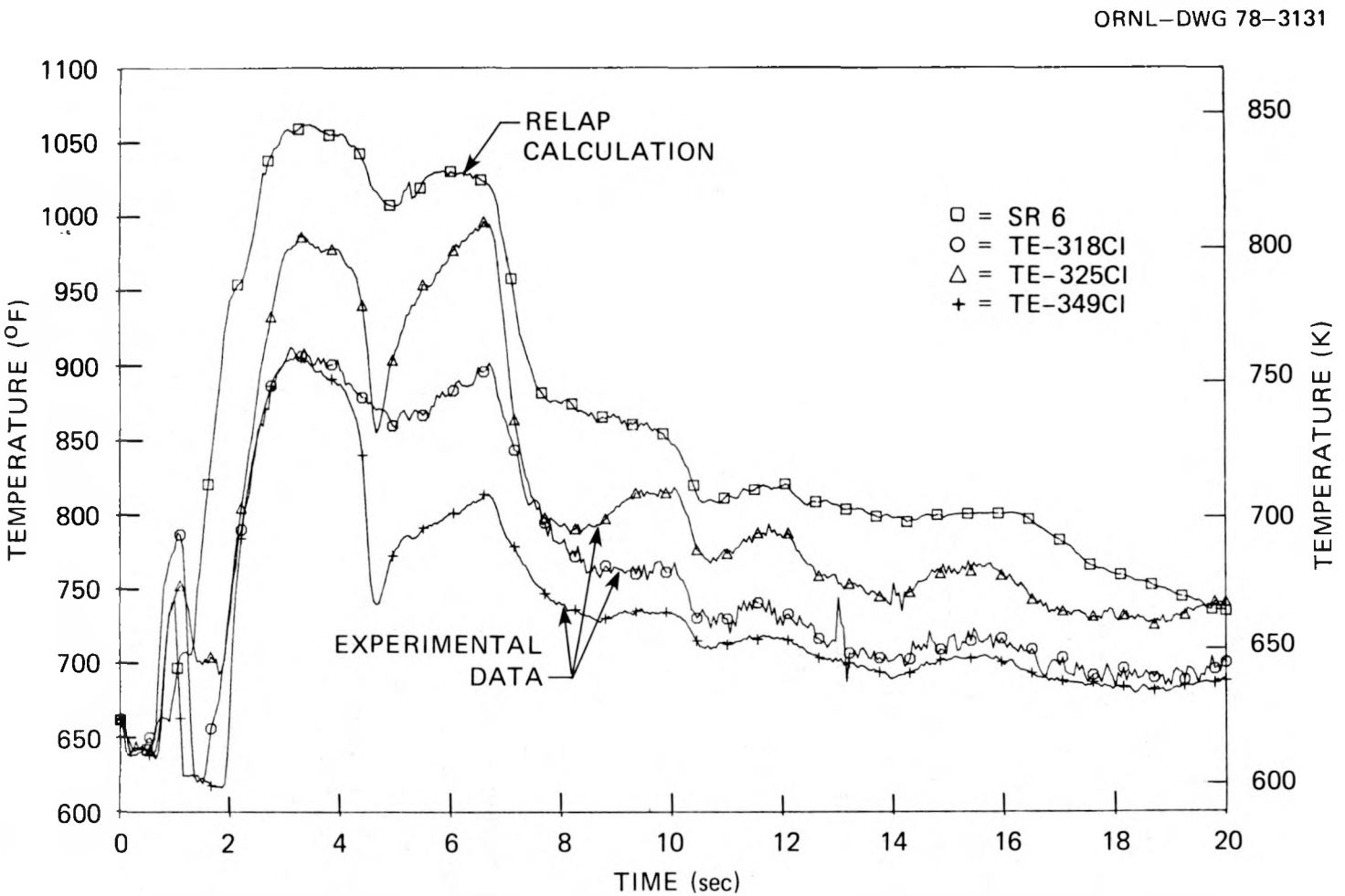

Fig. 2.7. RELAP-calculated rod surface temperatures compared to ORINC surface temperatures for rods 18, 25, and 49 at level I, test 105.

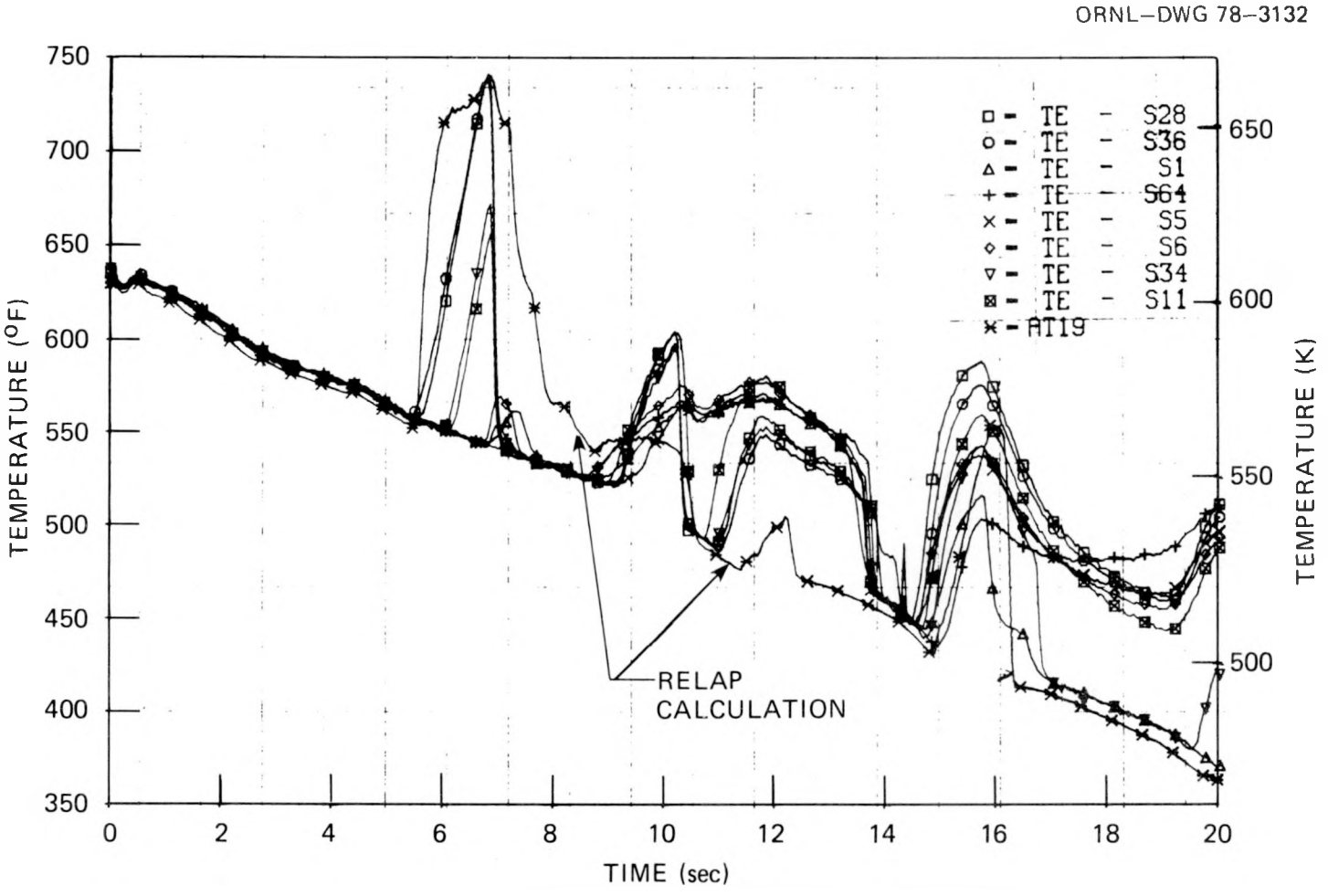

Fig. 2.8. RELAP-calculated fluid temperature and data from eight subchannel thermocouples during THTF test 105.

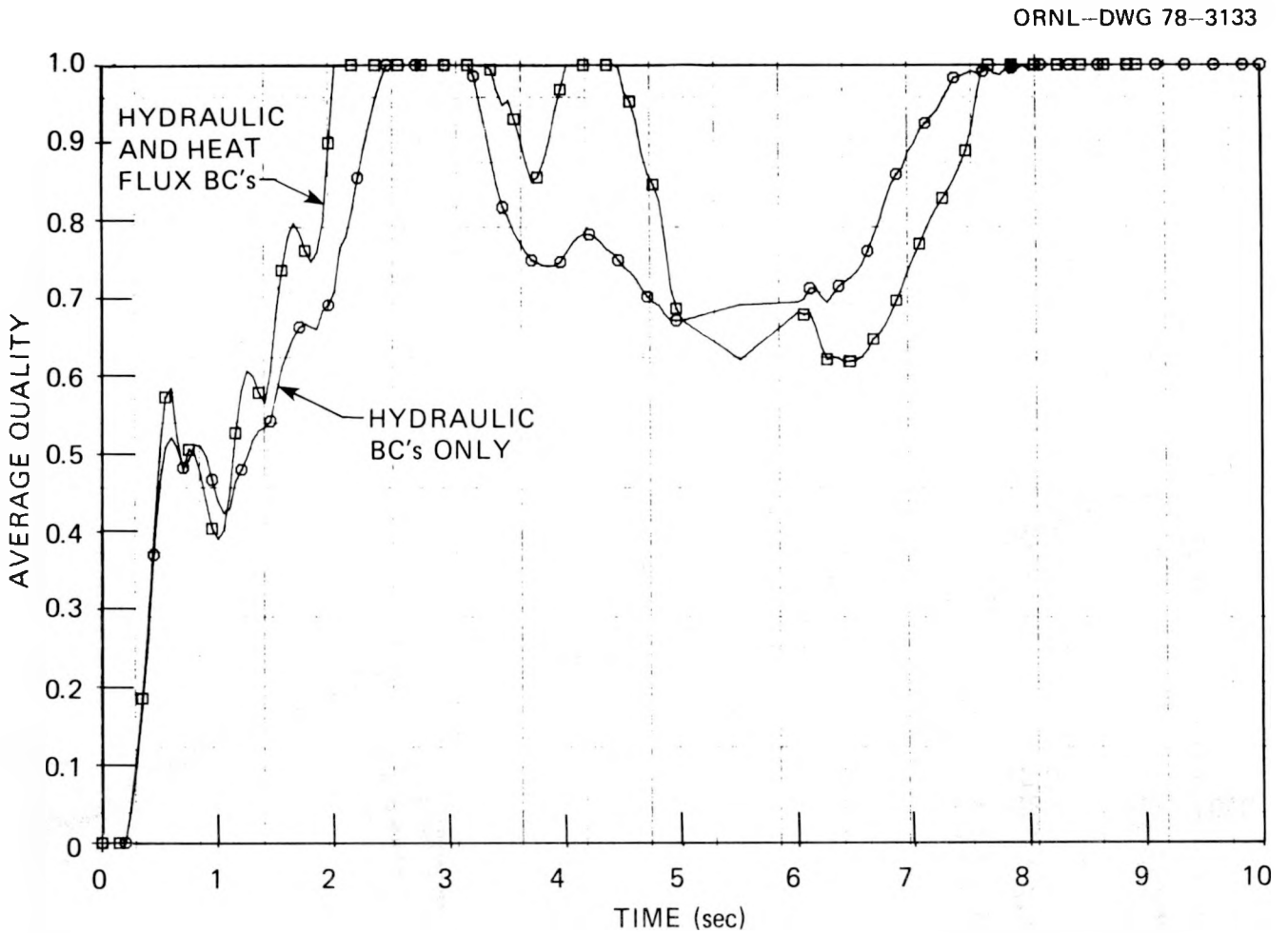

Fig. 2.9. Comparison of calculated fluid quality at bundle midplane using single-channel RELAP core model with hydraulic boundary conditions only (octagon) and with both hydraulic and heat flux boundary conditions (square).

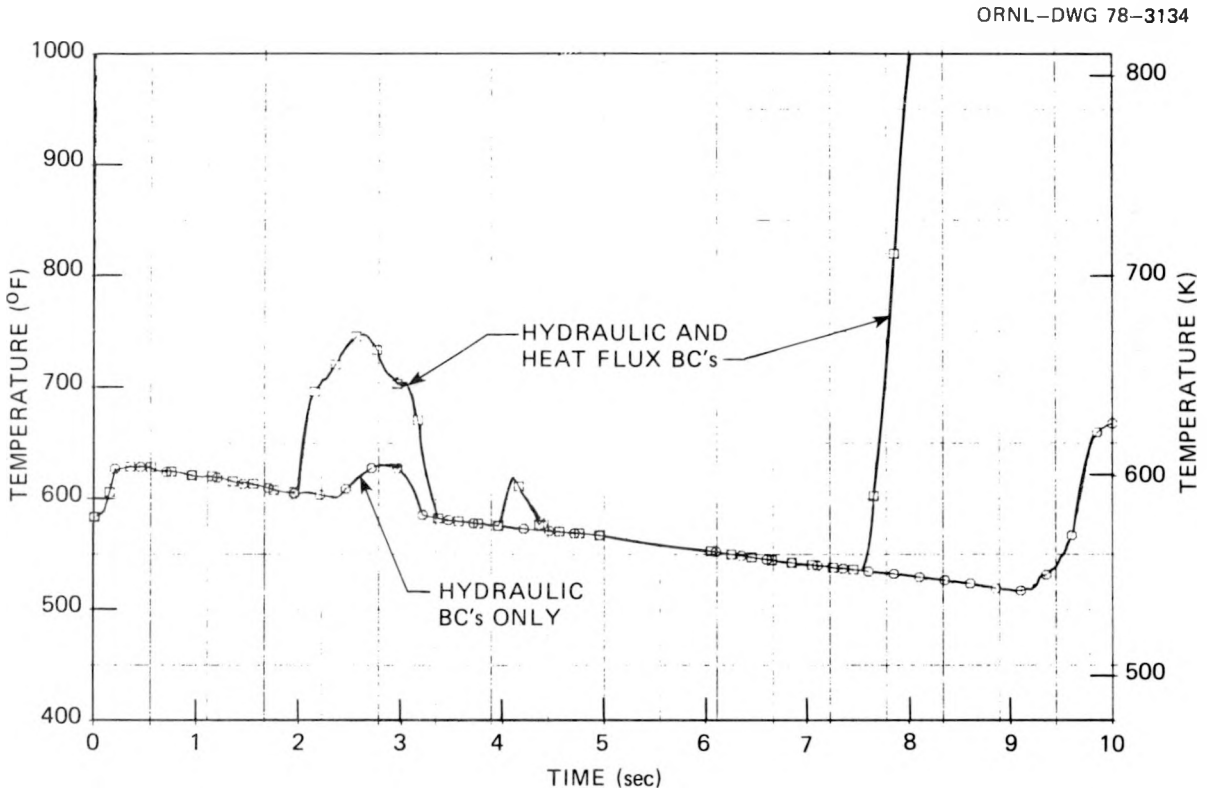

Fig. 2.10. Comparison of calculated fluid temperature at bundle midplane using single-channel RELAP core model with hydraulic boundary conditions only (octagon) and with both hydraulic and heat flux boundary conditions (square).

axial levels. However, due to the lack of fluid instrumentation in bundle 1, it will be difficult to estimate the error in fluid properties such as flow rate and enthalpy where the heat transfer coefficients are calculated.

Analysis of the FCTF with RELAP4 is continuing. Present indications are that RELAP predicts the system hydraulic response of the FCTF generally well. Comparison of RELAP's calculations to date are shown in Figs. 2.11, 2.12, and 2.13 for pressure, temperature, and density, respectively. Times to critical heat flux (CHF) have been more difficult to predict correctly; CHF times are typically several seconds in the FCTF (Fig. 2.14).

Figure 2.15 shows the primary modes on interaction of the Thermal Hydraulic Simulation Task Group with other groups in the Blowdown Heat Transfer (BDHT) Analysis Group and with BDHT Program Planning and Management.

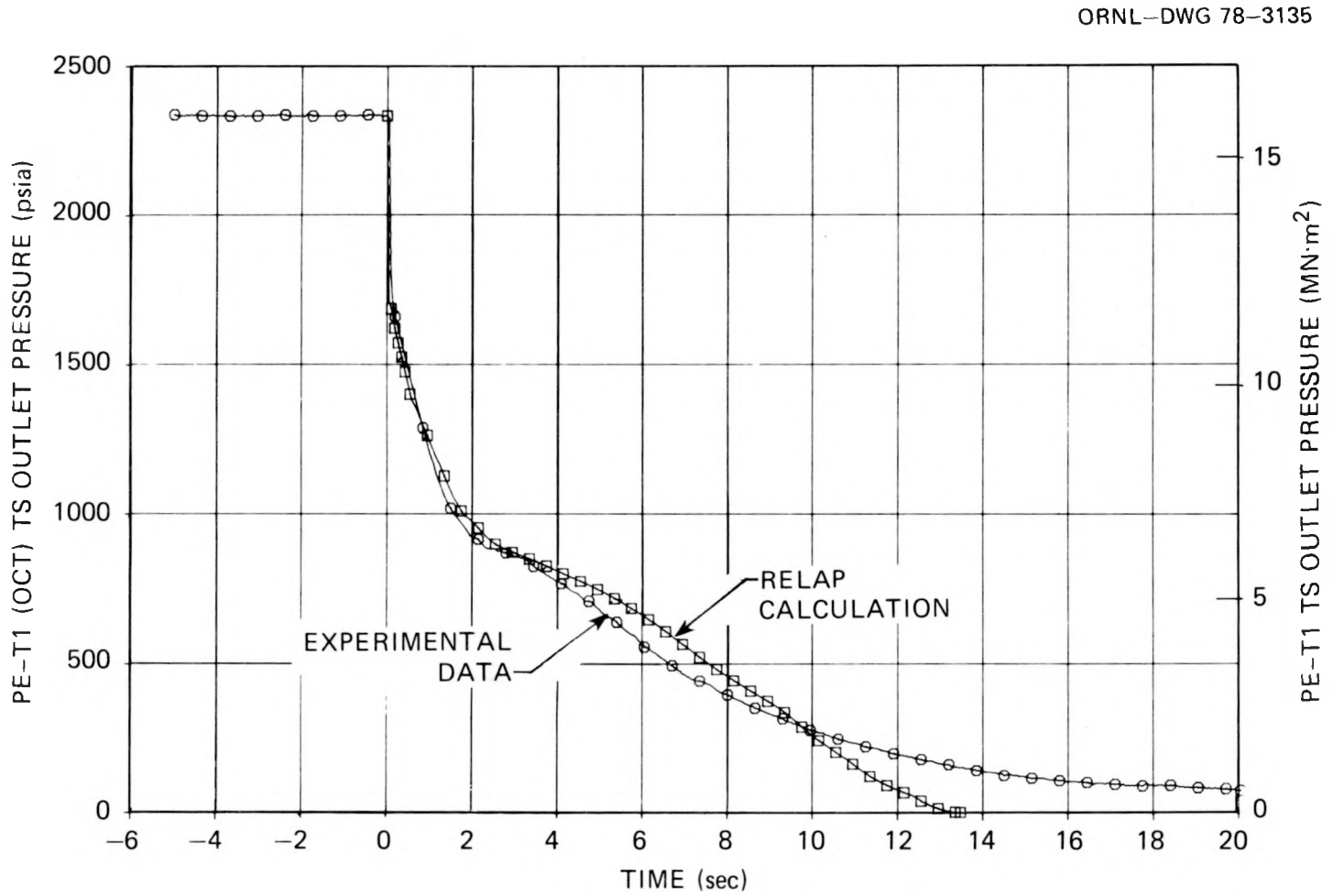

Fig. 2.11. RELAP-calculated and -measured pressure at FCTF test section outlet for test 77-1-3.

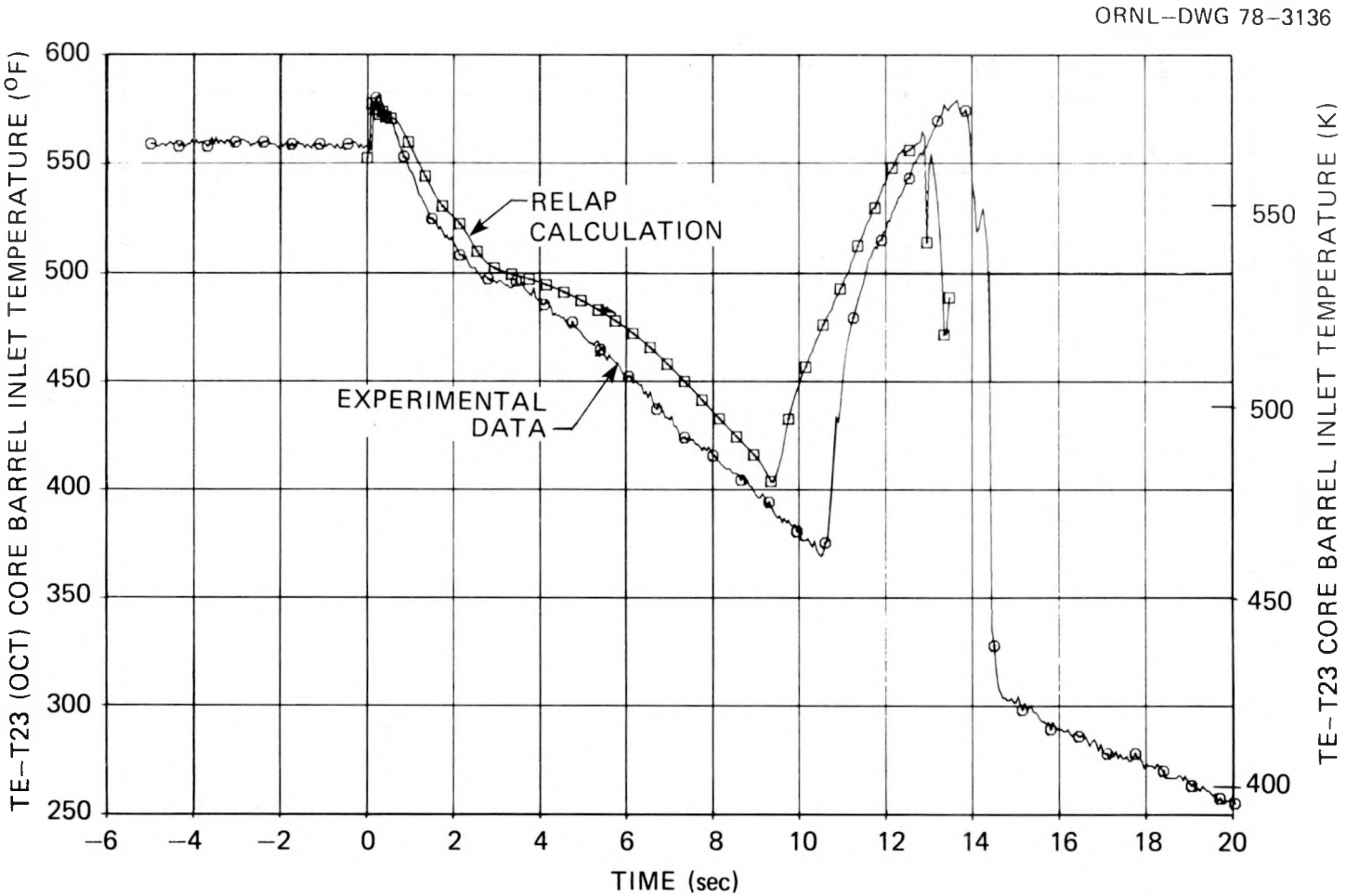

Fig. 2.12. RELAP-calculated and -measured fluid temperature at FCTF core barrel inlet for test 77-1-3.

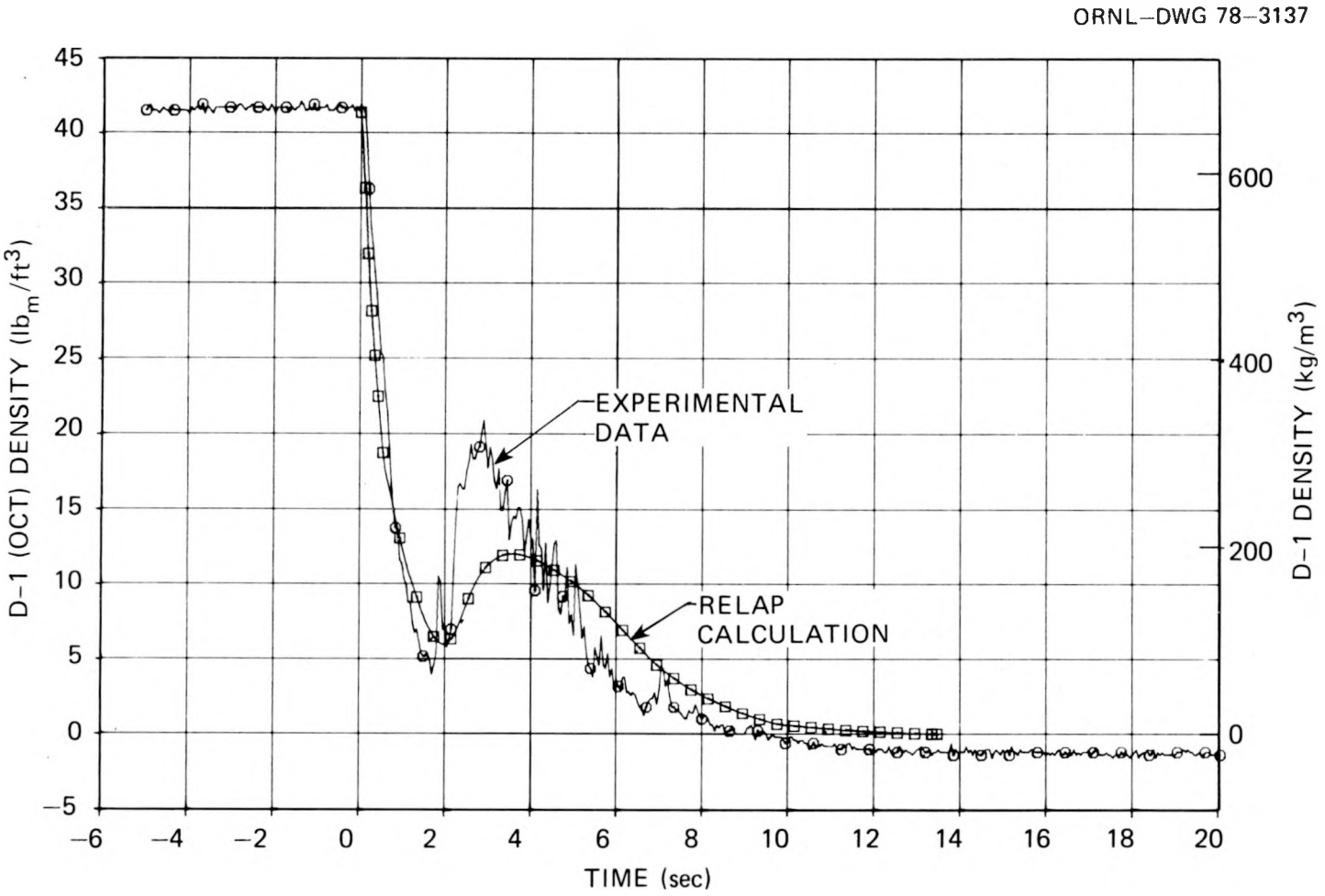

Fig. 2.13. RELAP-calculated and -measured density in FCTF hot leg for test 77-1-3.

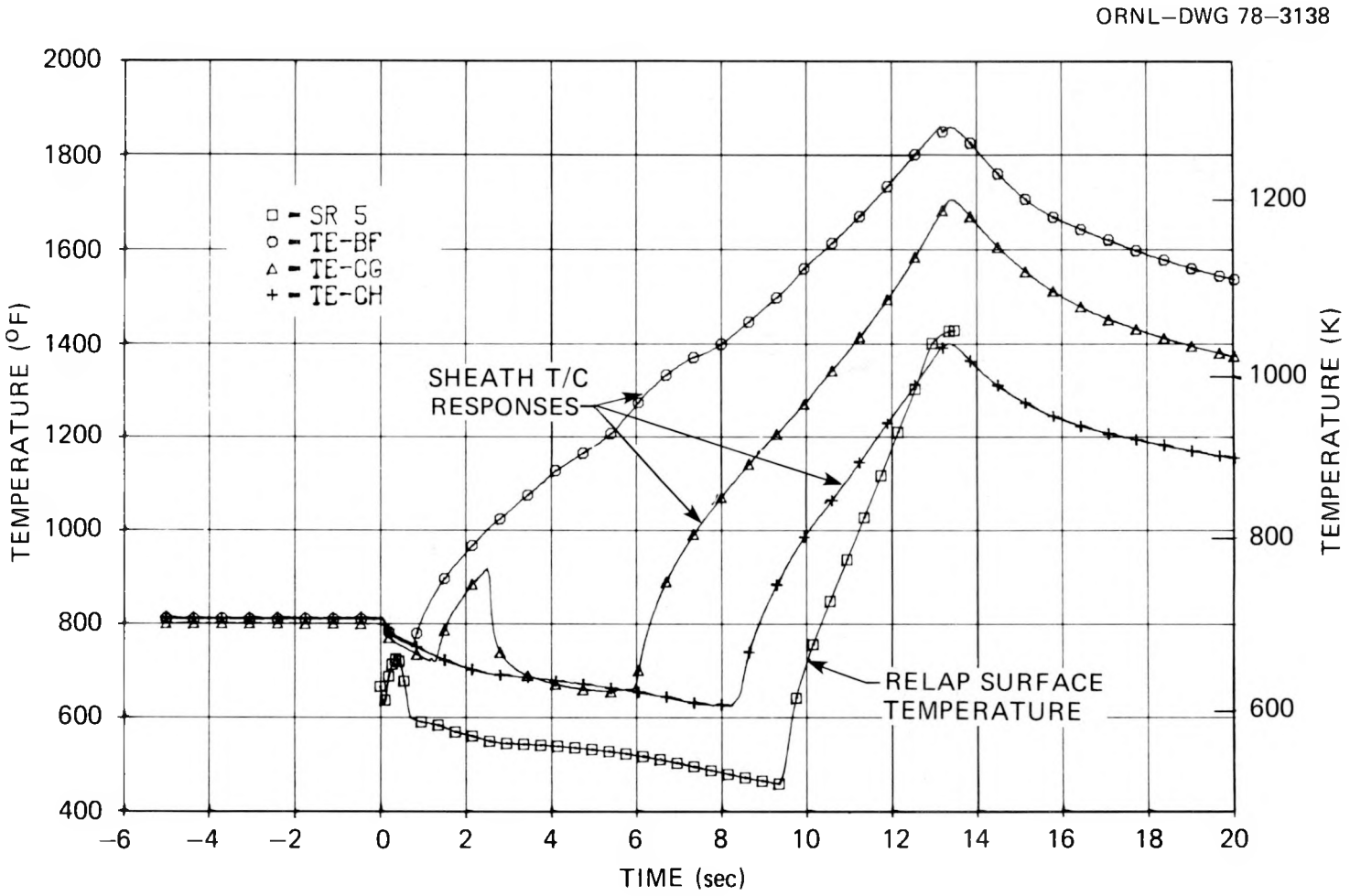

Fig. 2.14. Comparison of RELAP-calculated heater surface temperature in FCTF peak power zone with sheath thermocouple responses at levels F, G, and H (test 77-1-3).

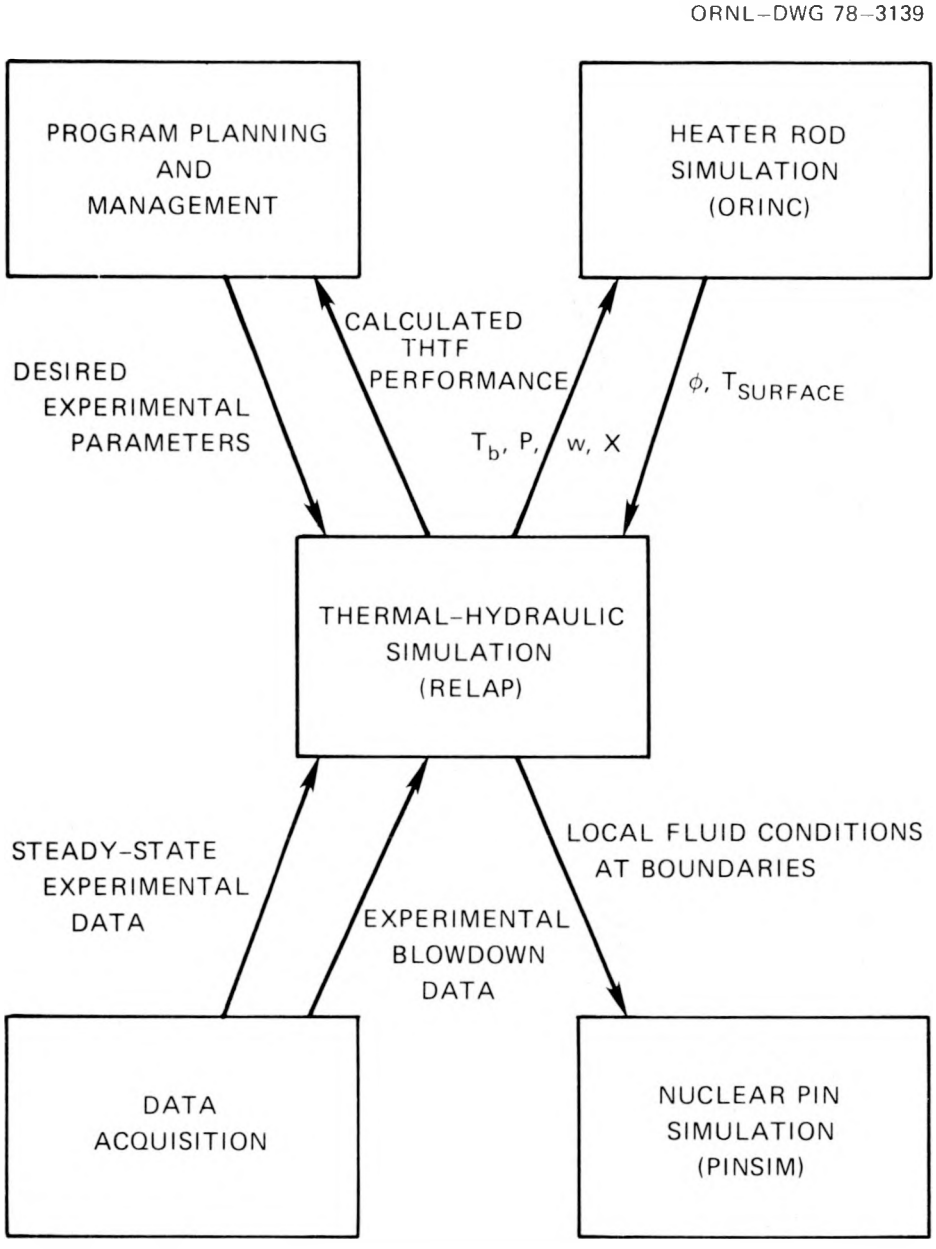

Fig. 2.15. RELAP task group interaction with other task groups.

3. THERMAL-HYDRAULIC TEST FACILITY OPERATION

R. E. Bohanan A. N. Smith

Blowdown tests 163, 164R, and 165 were conducted during this period, bringing the total power rod blowdowns to 20 for bundle 1. A summary of the heater rod experience is shown in Table 3.1. Attempts to conduct two other tests were unsuccessful. Test 164 failed due to a pump seal failure. Test 166 was delayed due to a pump bearing failure and subsequently rescheduled until after the fifth Water Reactor Safety Research meeting.

Table 3.1. Summary of THTF bundle 1 heater rod experience through test 165 (Oct. 13, 1977)

Item	This report period	Total
Hours at 0–30 kW/rod	2.6	88.1
Hours at 40–90 kW/rod	4.6	65.2
Hours at 100–122 kW/rod	1.2	21.9
Total powered hours	8.4	175.2
Hours at full power (122 kW/rod)	0	10.4
Number of blowdowns	3	21[a]
Heater rod failures	0	2[b]

[a] Includes isothermal test 171.

[b] Rods 39 and 47 with low resistance from heater element to ground. Failure discovered after a power outage during initial portion of test 106.

3.1 Pump Seal and Bearing Performance

The Bingham pump operated satisfactorily through test 163. During preliminary operations for test 164, however, the seals developed excessive leaks and were changed. Newly designed seals from Durametallic that used WC-graphite were then installed in both cavities and operated satisfactorily prior to test 164. At near blowdown conditions for this test, however, the outboard seal suddenly developed a severe leak, and within

seconds it failed completely. The rotating tungsten carbide ring had fractured into several pieces which damaged the pump seal cavity and the seal.

When the outboard journal bearing was removed to replace the outboard seal, the bearing was found to be badly damaged. Since no prior indication of pump problems was observed before the seal failure, the damage probably occurred when the seal failed. Subsequent replacement bearings also failed due to graphite in the oil. When the seal failed, steam entered the bearing housing, bringing with it graphite particles from the destroyed stationary seal ring. Normal cleaning apparently did not remove these particles, and they continued to mix with new oil and to act as an abrasive. The housing was steam-cleaned, and operation returned to normal.

3.2 The dc Power System Operation

The condition of the four dc generators continues to deteriorate. An extensive cleaning during November failed to alter the situation significantly (Tables 3.1 and 3.2). Resistance measurements on the motor-generator (M-G) sets (Figs. 3.1 and 3.2) are still very low.

Table 3.2. Summary of THTF primary pump seal performance through Nov. 4, 1977

Seal design	Seal location	Mating surfaces	Number of blowdowns	Total hr operating
Durametallic	Outboard	WC-WC	6	369
Borg-Warner	Inboard	WC-WC	0	3
Durametallic	Inboard	WC-WC	6	326
Borg-Warner	Outboard	WC-graphite	2	86
Borg-Warner	Inboard	WC-graphite	0	29
Durametallic	Outboard	WC-WC	4	97.4
Durametallic	Inboard	WC-WC	5	111.4
Durametallic	Outboard	WC-WC	4	79.2
Borg-Warner	Inboard	WC-graphite	9	153.6
Borg-Warner	Outboard	WC-graphite	6	88.4
Durametallic	Inboard	WC-carbon	0	8.4
Durametallic	Outboard	WC-carbon	0	8.1
Borg-Warner	Outboard	WC-graphite	2	23.2
Durametallic	Inboard	WC-WC	2	34.5
Durametallic	Outboard	WC-WC	0	11.6

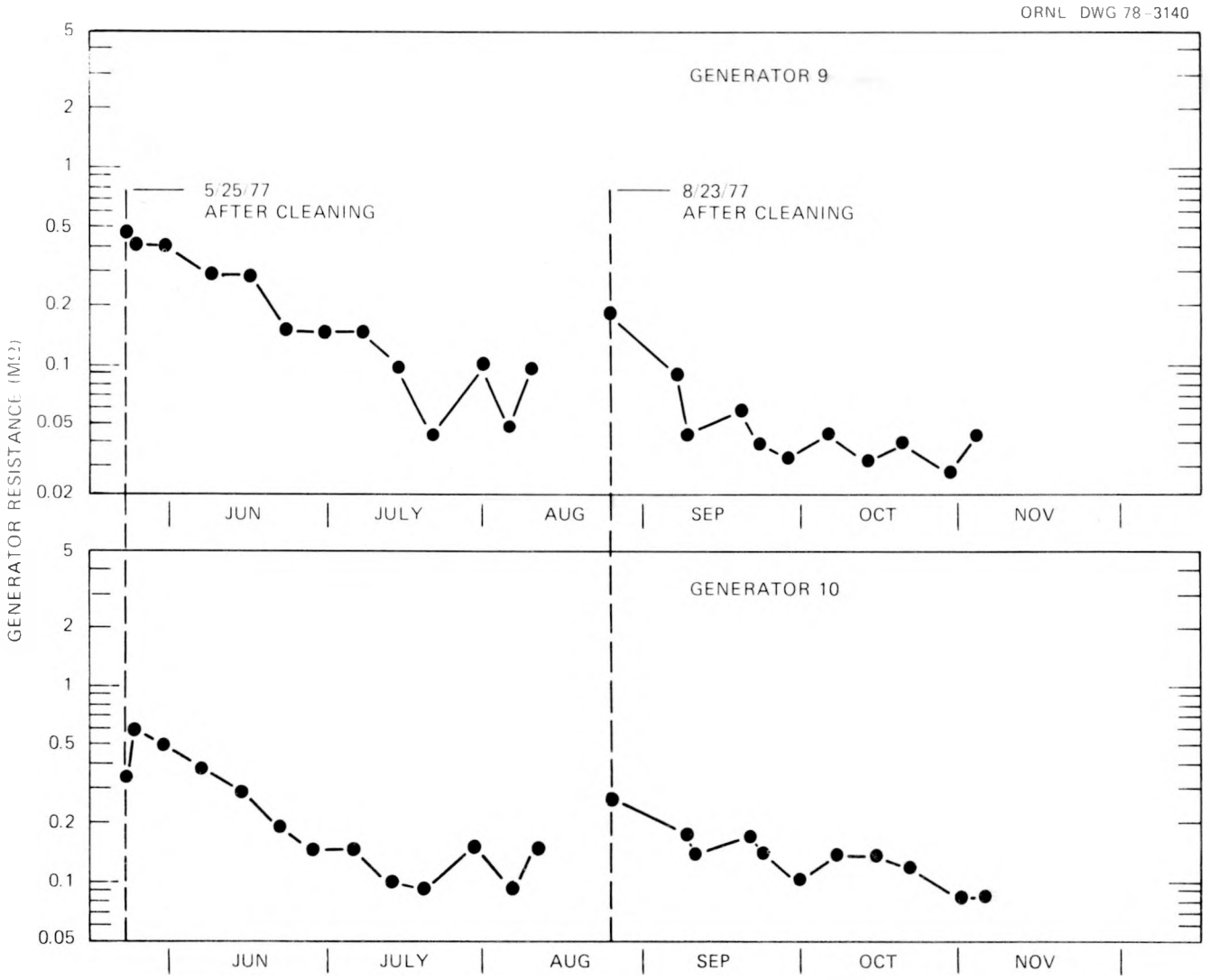

Fig. 3.1. Resistance readings on M-G sets 9 and 10.

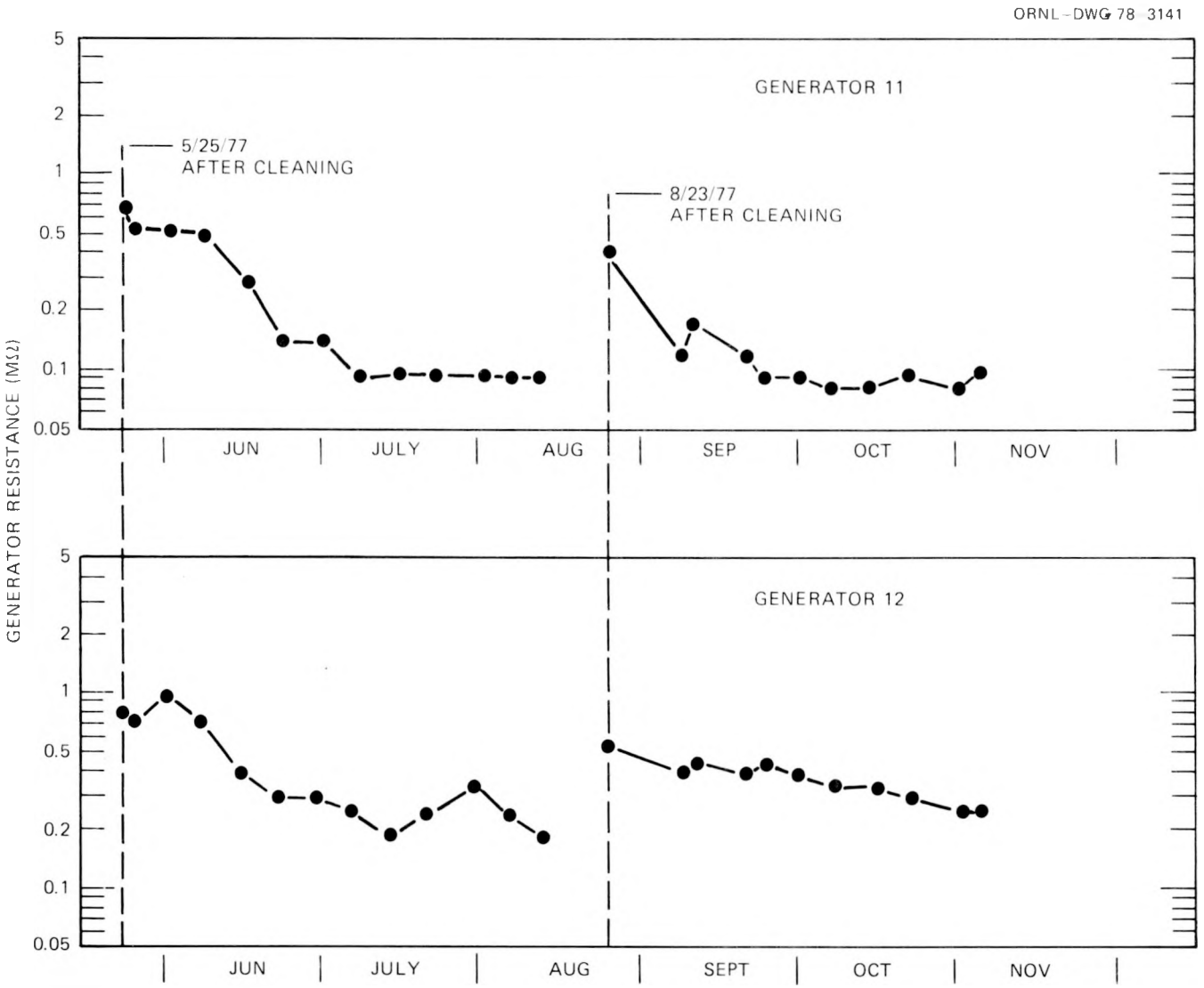

Fig. 3.2. Resistance readings on M-G sets 11 and 12.

Prior to each operation of the THTF, the machines are tested for current leakage to ground. The complete machines are subjected to 250 V to ground, and the current is monitored. If the current remains small (<10 mA) and constant, the generator's internal resistance to ground is assumed to be uniform throughout. A concentrated low-resistance point could result in a high current and cause damage. During this test the machine is protected with a 1/4-A fuse.

Progress has been made toward rebuilding the spare motor generator set. Purchase requisition No. Q06780 was sent to Purchasing this quarter, and a contract is expected to be signed in January 1978, with delivery in June 1978.

3.3 THTF Bundle 3 Modification

Bundle 3 is a 64-pin bundle, 60 heated rods and 4 instrument rods. These additional rods will require a substantial redesign of the dc power distribution and protective system. This redesign is underway and should be completed by March 1978. The bundle design is complete for comments.

A feature unique to this bundle is the rod upper O-ring seal. Previously, the O-ring has been in the housing around the rod, making it almost impossible to change a rod with the bundle in the test section because of extreme difficulty in replacing the O-rings. The new design has the O-ring and groove on the rod so that rod and O-ring may be replaced without removing the bundle from the test section.

3.4 THTF Control Room Addition

Phase I (the floor, walls, doors, and roof) is complete. The start of Phase II (the heating and ventilation, fire protection, general electric services, and the interior) was delayed due to funding problems. The scope of the cost-plus-fixed-fee (CPFF) contractor's work was reduced to installation of the heating and ventilation system and the fire protection system. The CPFF work should be finished in January 1978. The BDHT personnel will finish the remainder through Y-12 Maintenance.

3.5 Periodic Instrument Recalibration

The THTF is a heavily instrumented facility. Many of these instruments are checked for calibration prior to each test. About 125 do not require calibration this frequently, but they do require a periodic calibration to maintain a high-quality standard. To ensure this standard, these instruments have been entered into the Y-12 computer-controlled calibration recall program. The THTF operating crew is notified about three weeks prior to the date prescribed for recalibration, and plans are made for this recalibration.

4. TWO-PHASE FLOW INSTRUMENTATION

I. T. Dudley
C. D. Griffies
P. H. Hayes
P. A. Jallouk
A. F. Johnson*
W. Ragan*
B. J. Veazie*

4.1 EG&G Liquid-Level Detector System Performance Tests in the FCTF

The liquid-level detector system which was purchased from EG&G Idaho, Inc., for use in the BDHT Program here at ORNL was delivered and tested in the FCTF. This level-detection system consists of an assembly of 19 sensing elements mounted in a probe plus an electronics package which provides signal conditioning, signal readout, and an output signal for the data acquisition system.

The probe sensing elements consist of small electrodes surrounded by cylindrical ground planes. The presence or absence of liquid at each sensing element is detected by measurement of the electrical conductivity between the electrode and ground plane.

The probe assembly was designed specifically for use in the THTF fuel pin simulator bundle 2 and will be used for determining the location of the liquid-vapor interface in experiments which simulate loss-of-coolant accidents in a pressurized-water reactor. Overall length of the probe is 637.2 cm (250.9 in.). The 19 sensing elements spaced approximately 17.8 cm (7.0 in.) apart are mounted in a stainless steel tube 1.392 cm diam (0.548 in.) by 417.2 cm long (164.25 in.). Closely spaced slots were cut in the wall of the tubing to provide free passage of the steam and liquid coolant past the sensing elements. A portion of the liquid-level device is shown in Fig. 4.1. The outside diameter of the tubing at the upper end of the probe (Fig. 4.2) was reduced to 1.21 cm (0.476 in.) to accommodate the O-ring seals to be used in THTF bundle 2.

The electronic signal conditioning package for the liquid-level probe drives each probe with a square wave of constant current and monitors the voltage signal as measured across the probe. The peak voltage of the signal

*Instrumentation and Controls Division.

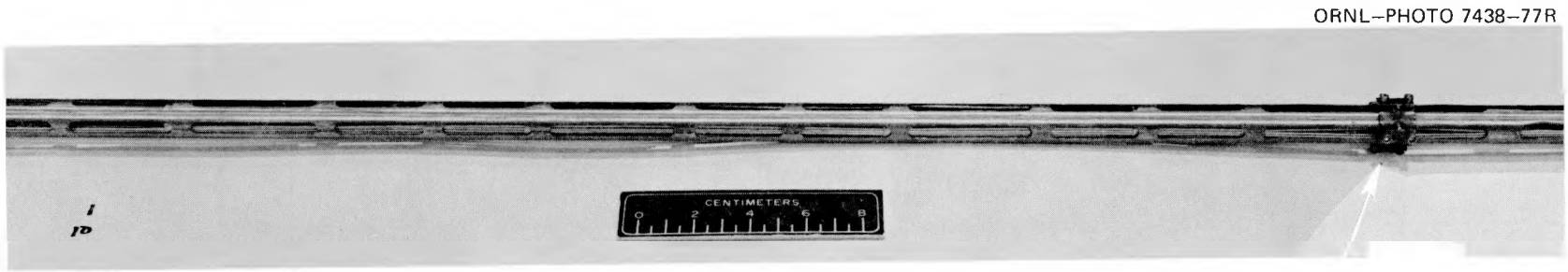

Fig. 4.1. Liquid-level probe with spacer attached.

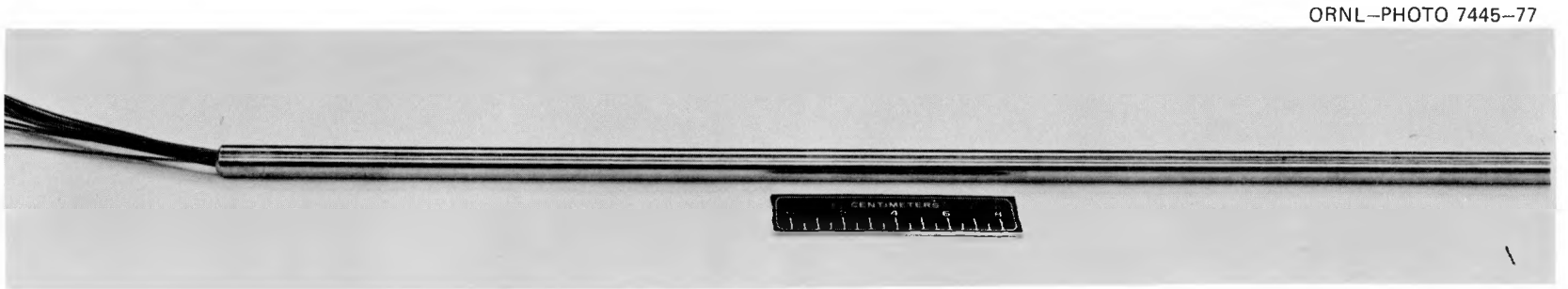

Fig. 4.2. Liquid-level probe — upper end.

(which is also a filtered or unfiltered square wave) is then inversely proportional to the conductivity of the fluid at that point. A comparator then compares the peak voltage signal against a threshold setting to determine if that point is water (high conductivity) or not water (low conductivity). Both the probe output signal (analog) and the water/no-water signal (binary or bilevel) are available for recording. The threshold setting can be determined in either of two ways: manually or from an average of the lower N probes, which are assumed always to be wet. If the bottom probes do dry out, an override setting automatically switches to the manual threshold.

The main objectives of testing the liquid-level probe in the FCTF were to verify the integrity of the device before installation in bundle 2 and to evaluate the performance of the probe using demineralized water. The INEL facilities using similar probes increase the conductivity of their water with additives such as lithium hydroxide in order to better discriminate the water and steam phases. However, the inclusion of additives in the water changes its heat transfer properties such that the BDHT program would prefer to continue with the demineralized water presently in use. Since the conductivity of water is strongly a function of temperature (increasing as the water temperature increases), these tests have indicated that water at the nominal THTF blowdown temperature of 286°C (547°F) should have high enough conductivity to be reliably discriminated from steam.

Prior to installation in the FCTF, special precautions were observed during all phases of the handling of the probe assembly to protect it from damage, including the use of special tables and upending fixtures. In addition, to provide lateral support and therefore prevent the probe from bending in the FCTF core barrel during a blowdown, seven small spacers were temporarily mounted on the probe assembly. An example is shown in Fig. 4.1. These spacers were located at approximately the same positions that the grid spacers of THTF bundle 2 would contact the probe. The locations were 34.3 cm (13.5 in.), 101.6 cm (40.0 in.), 153.2 cm (60.3 in.), 214.6 cm (84.5 in.), 274.6 cm (108.1 in.), 339.1 cm (133.5 in.), and 398.8 cm (157.0 in.) from the lower end of the probe assembly. All spacers were slid axially over the probe and then locked in position by small screws which extended into the ends of adjacent slots. In this manner, each

spacer was secured to the probe without damage or alteration to the probe itself. Diametral clearances of 0.079 cm (0.031 in.) to 0.159 cm (0.062 in.) between the inside of the FCTF core barrel tube and the screw heads on the spacers were provided by arrangement.

Since it was not possible to pass the bundle of 19 coaxial cables attached to the lead wires from the probe through the O-ring seals in upper flange assembly of the FCTF, it was necessary to remove all of the coaxial cables and junctions from the sheathed lead wires. The sheathing was then stripped from each lead for approximately 2.5 cm (1 in.), heated for drying purposes, and then resealed with epoxy cement. After the bundle of lead wires was passed through the O-ring seals of the flange assembly, each lead wire was attached to a small terminal board. This same procedure was found to be satisfactory and will be used when installing the probe assembly in THTF bundle 2.

The probe assembly was visually inspected prior to installation and testing in the FCTF. Some ripples were observed in the upper end of the slotted tube which contains the sensor elements. These ripples may be seen in Fig. 4.3.

After the liquid-level device was installed in the FCTF, the system was charged with demineralized water which had a conductivity at room temperature of less than 1 micromho.

The first set of evaluation tests run were fill/drain tests at up to approximately 369 K (205°F). The difference in conductivity between the demineralized water and air was not sufficient to reliably discriminate the two in all cases. Next, a series of three blowdown tests was run as shown in Table 4.1. The tests represented fast, slow, and intermediate speeds as determined by the blowdown orifice size.

The response of the liquid-level system during blowdown test 1 is shown in Fig. 4.4. For each of the 19 probes, if the bilevel output indicated water, a solid line is shown at that level for that time state. Thus, in effect, the presence of water is indicated by the shaded areas. The bilevel signals are updated every 100 msec, which is then the effective time resolution of the plot. As can be seen, the test section emptied beyond the active length of the level probe in 200 msec. The probe output signals for three levels are shown in Fig. 4.5. The change in

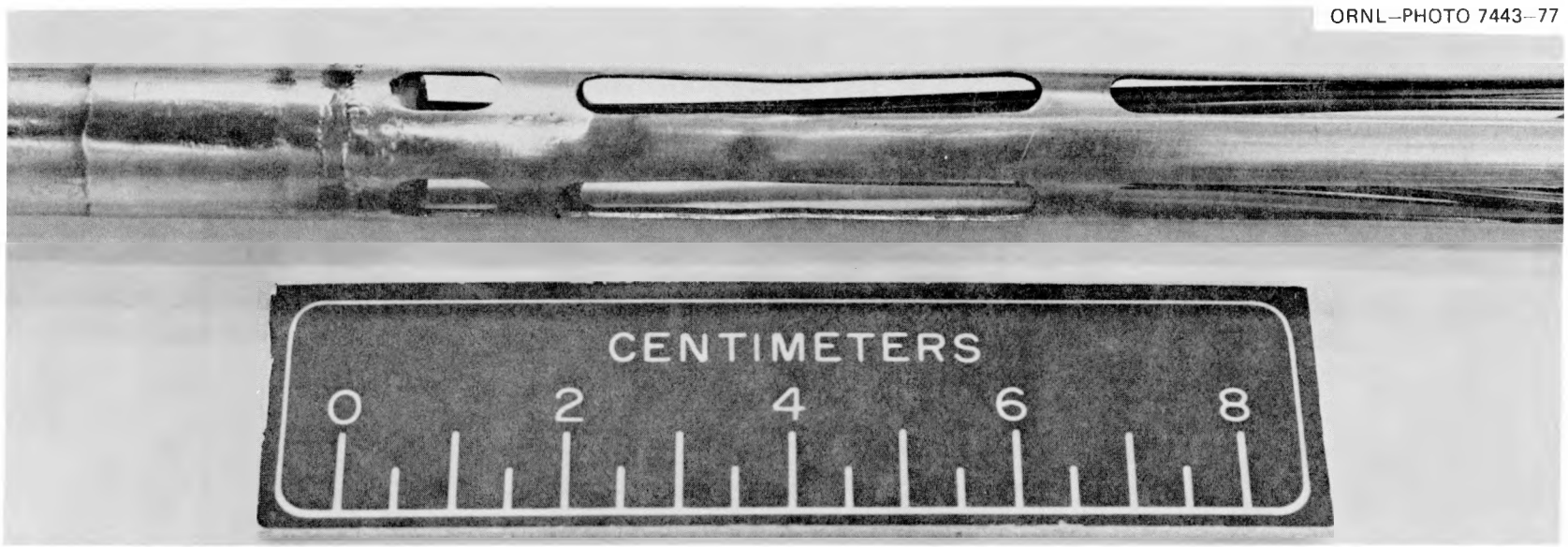

Fig. 4.3. Liquid-level probe — upper end of slotted tube section.

Table 4.1. Blowdown tests of EG&G liquid-level probe[a]

Test	Blowdown orifice diam [mm (in.)]	Typical probe output signal levels	
		Preblowdown (V peak)	Postblowdown (V peak)
1	24.6 (0.970)	0.9	8.7
2	5.33 (0.210)	0.9	3.2
3	8.71 (0.343)	0.7	3.4

[a]All blowdowns were from nominal loop steady-state conditions of 505 K (450°F), 15.5 MN/m^2 (2250 psig), and 1.3×10^{-3} m^3/sec (20 gpm). The fluid was demineralized water in all cases.

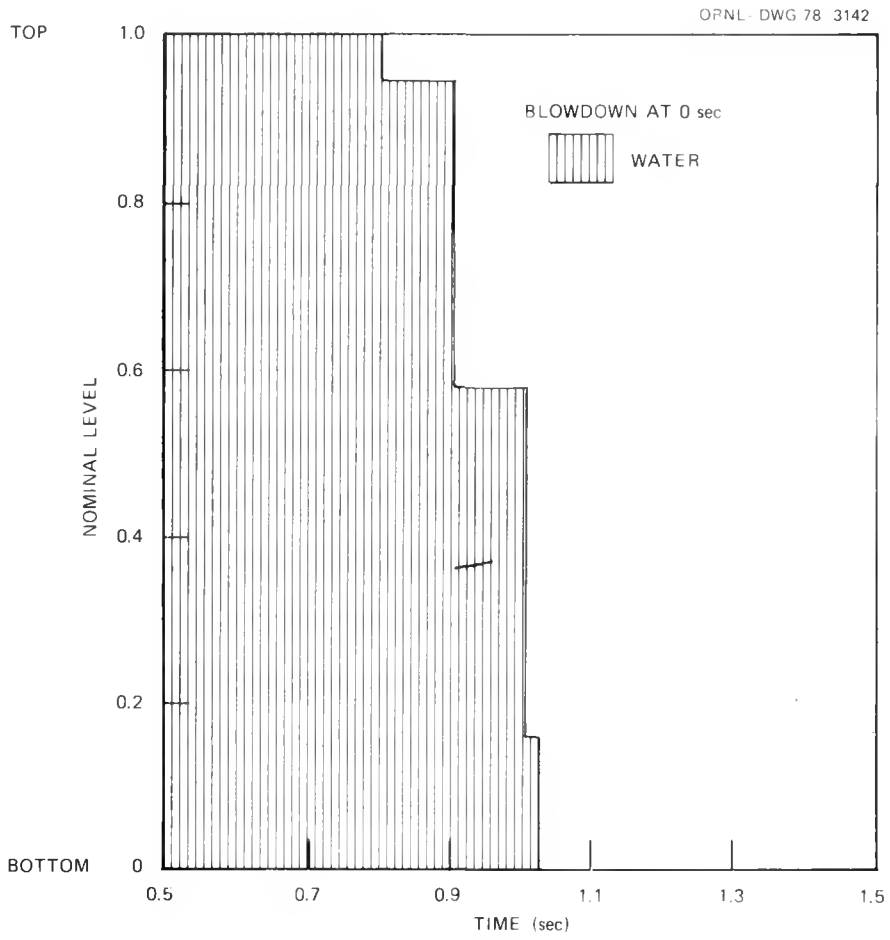

Fig. 4.4. Blowdown test 1 liquid level.

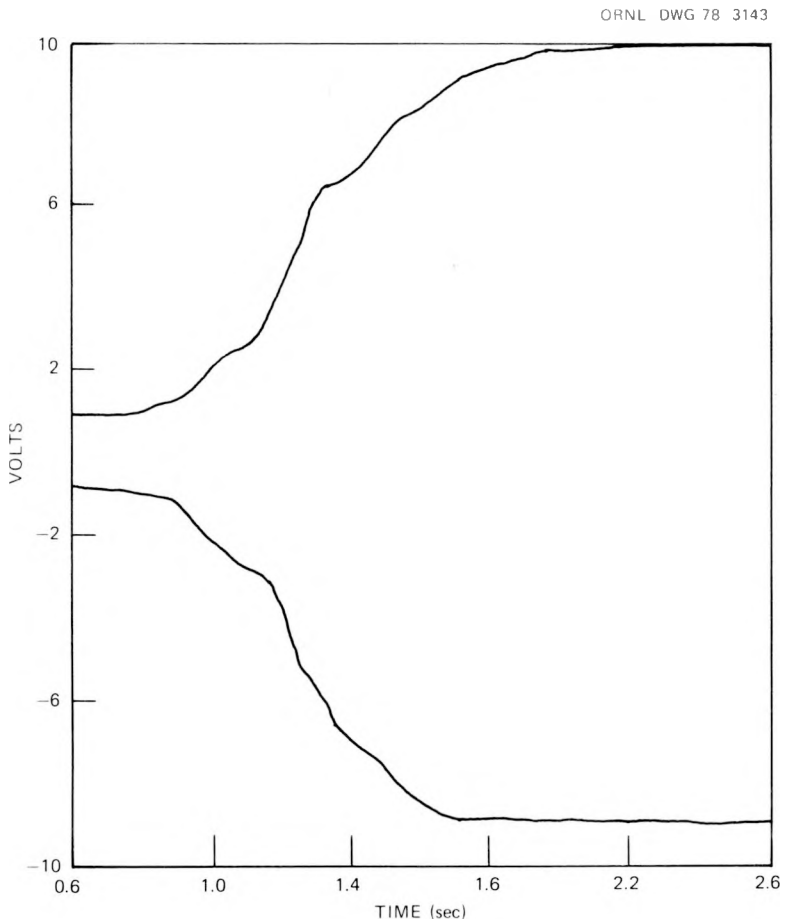

Fig. 4.5. Blowdown test 1 typical probe output signals.

signal level from wet to dry is on the order of 8 V, allowing easy discrimination between phases.

Blowdown test 2, a slow transient, is shown in Fig. 4.6. The partial emptying of the test section, discharge of the pressure water, and final emptying are clearly visible. Figures 4.7 and 4.8 indicate that the change in signal level is substantially reduced, on the order of 2.5 V. In fact, in Fig. 4.8, the demarcation between wet and dry is not obvious and can only be determined by comparing the output of the higher level probes to the output of the lowest probe(s), which are assumed to be wet. (This is, in fact, what the signal conditioner package does.) The apparent slugs of water after the test section has emptied (after about 9.0 sec) are probably due to those probe signals being just at the threshold of the comparator

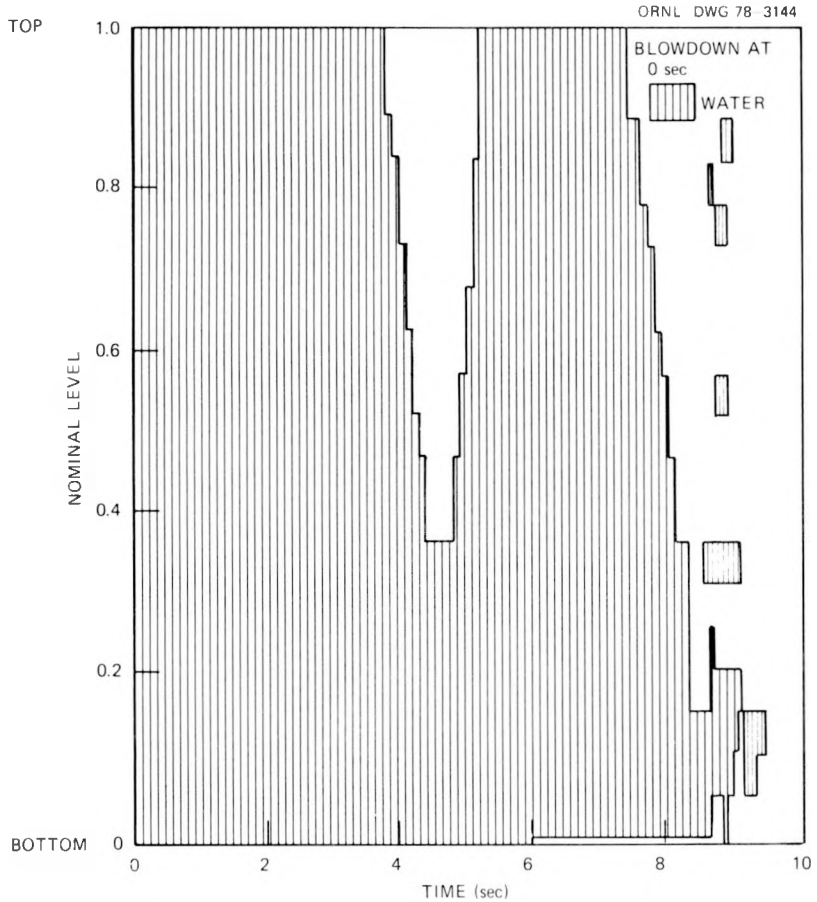

Fig. 4.6. Blowdown test 2 liquid level.

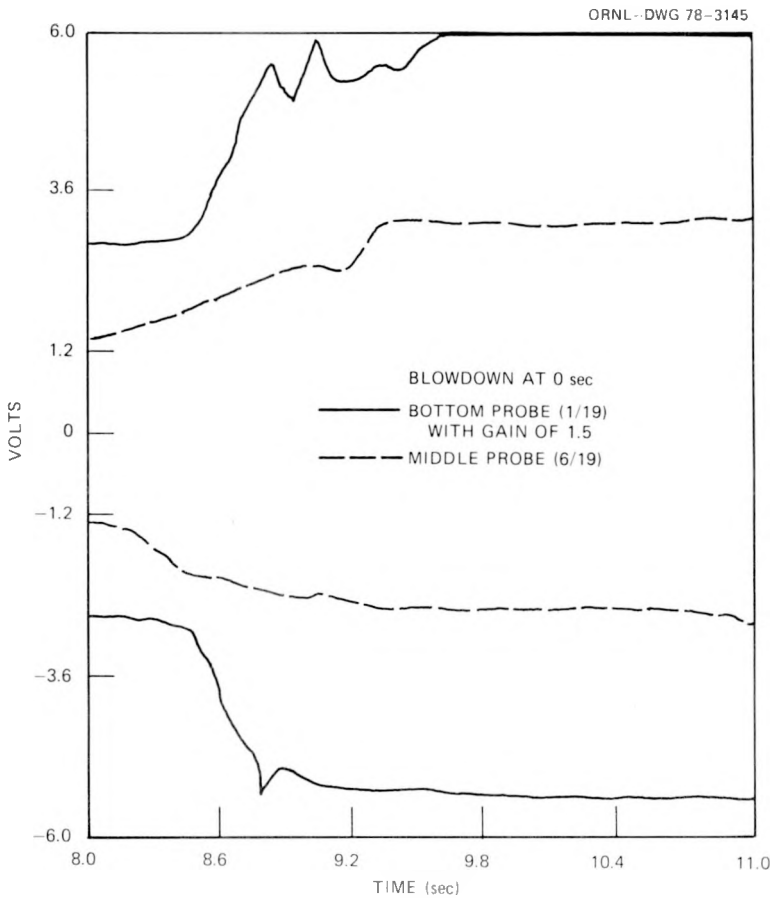

Fig. 4.7. Blowdown test 2 typical probe output signals.

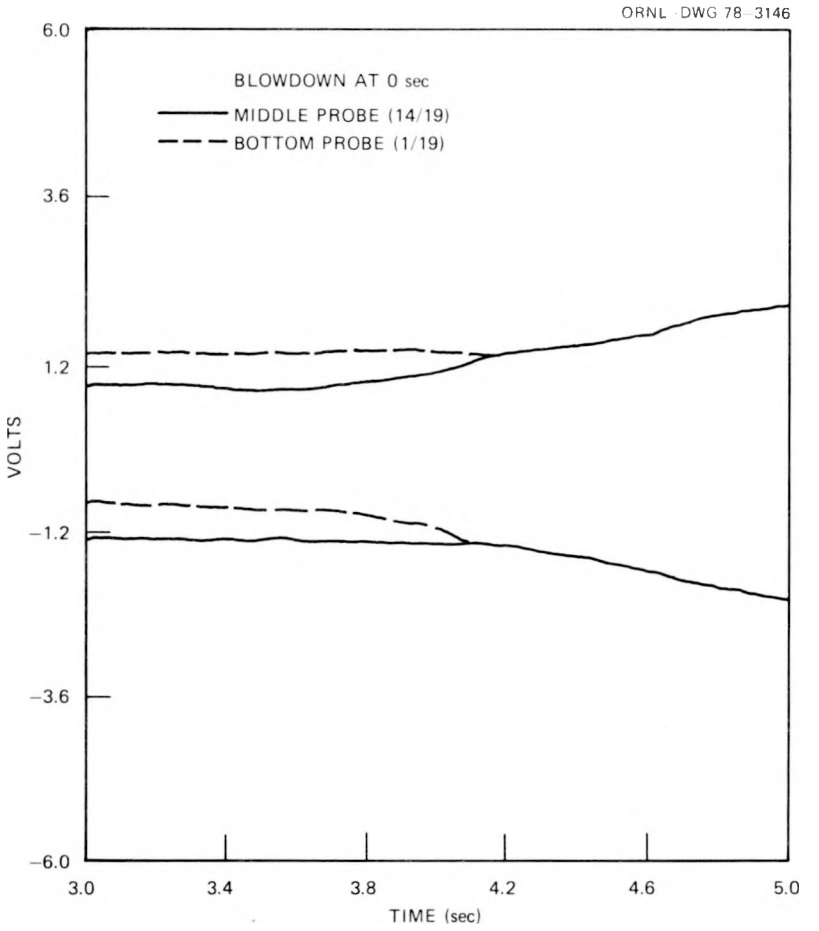

Fig. 4.8. Blowdown test 2 typical probe output signals.

when all probes went dry. Had the manual (override) threshold been set lower (as it should have been if the lower signal outputs had been anticipated), those slugs would not have appeared. The probable explanation for the lower dry signal output voltages for this test is a significant concentration of entrained steam in the test section. This condition contrasts with that of the first test, where the blowdown orifice was large enough to allow most of the water to flash to steam and be rapidly blown out.

Blowdown test 3 showed a similar, but faster, response to test 2 (Fig. 4.9). The probe output change was on the order of 2.7 V as shown in Fig. 4.10. Again, the slugs of water after 3.0 sec are due to a nonoptimum threshold setting.

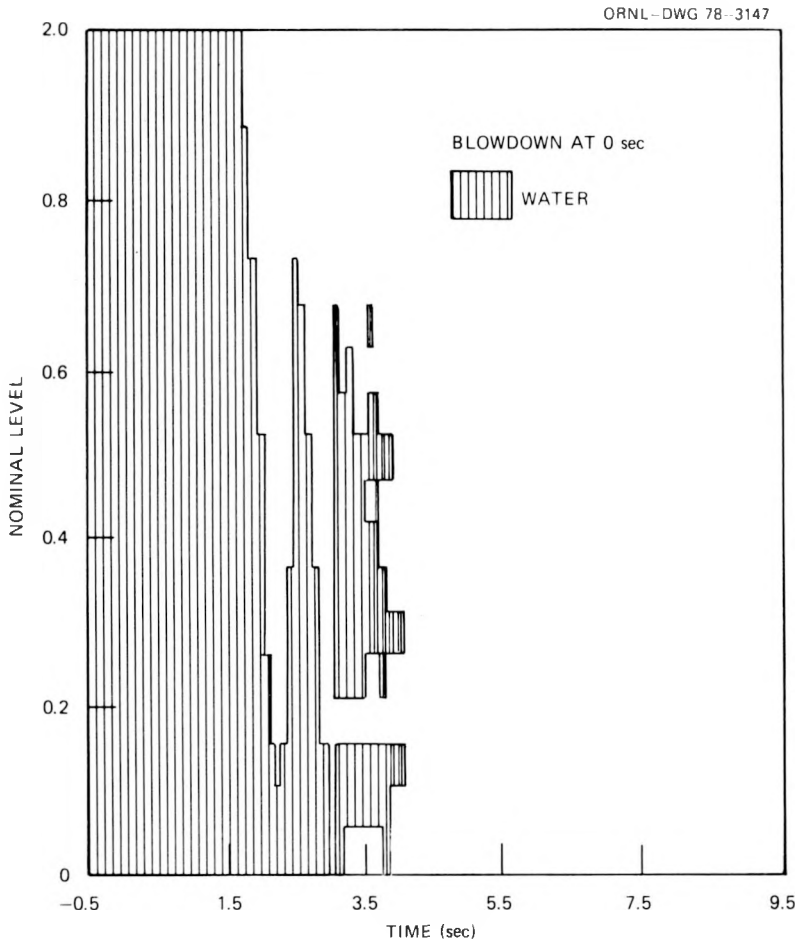

Fig. 4.9. Blowdown test 3 liquid level.

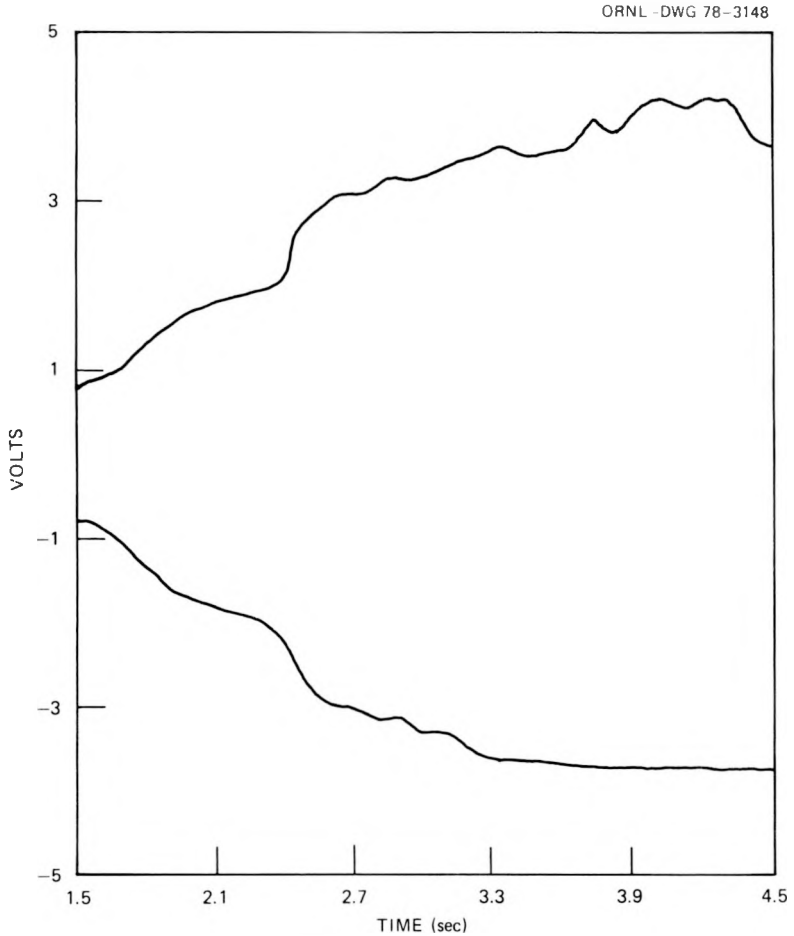

Fig. 4.10. Blowdown test 3 typical probe output signals.

In summary, the evaluation tests in the FCTF indicate that, with the proper threshold settings, the water/steam phases can be discriminated using demineralized water at the nominal blowdown temperatures of the THTF. It is evident, however, that the threshold settings are critical and may have to be optimized for each test depending on the loop response predicted. Further, in order to establish more confidence in the bilevel wet/dry signals, it will be very desirable to record the probe output analog signals for more detailed processing.

After the testing was completed, the liquid-level probe was removed from the FCTF and reinspected. No change in the probe's appearance was noted except for some discoloration of the metal in the high-temperature zone.

4.2 Horizontal Spool Piece Tests

J. E. Hardy P. A. Jallouk

A series of tests with a horizontal spool piece has been run in the air-water loop. Four 20-mesh screens and different sized ramp orifices have been used to homogenize the flow and to possibly improve the accuracy of the instrumentation. These tests were described in a previous quarterly report.[5] The results from the first two sets of runs made with and without the four 20-mesh screens will be discussed here.

The instrumentation used consisted of a drag disk, a turbine meter, a three-beam gamma densitometer, and an Auburn vapor fraction monitor. If homogeneous flow is assumed, any two of three instruments measuring different parameters can be used to determine the flow rate.[6] In Figs. 4.11 through 4.13, the flow rates from combinations of these instruments are compared with the true mass flow rate reading. Ideally, if the flow were homogeneous, the ordinate would have a value of unity at all values of quality. Figures 4.11 through 4.13 indicate that, with no screens, only at very few qualities is the flow actually homogeneous. At higher flow rates, the deviations can be quite large, and no one curve can be found to represent all flow rates.

When the Aya model is applied, three instrument readings (drag disk, turbine meter, and void fraction) are needed. The plot obtained in Fig. 4.14 with the Auburn meter void fraction indicates that a considerable

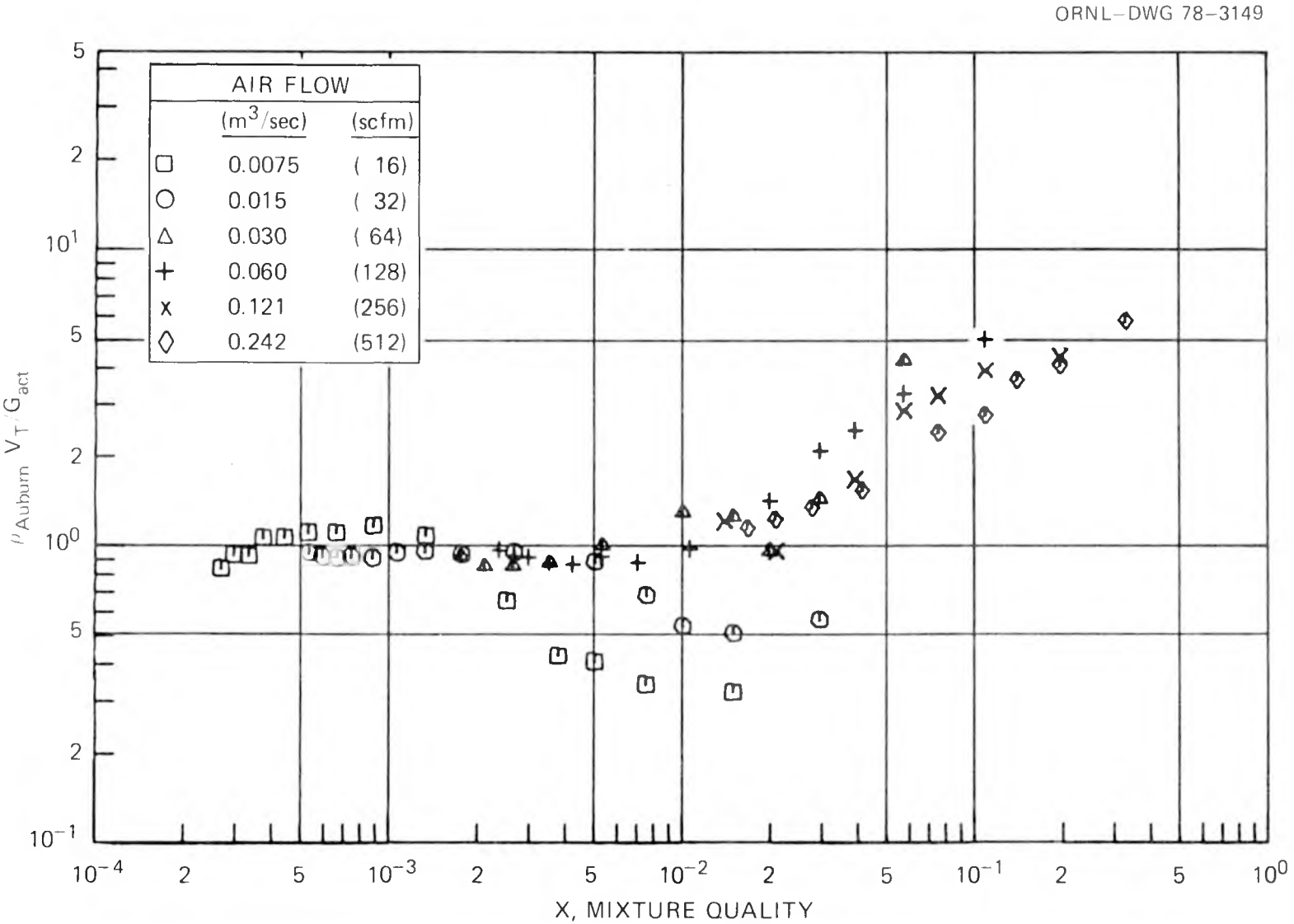

Fig. 4.11. Variation in the mass flow rate calculated using the one-velocity $G = \rho_{Auburn} V_T$ model as a function of mixture quality — no screens.

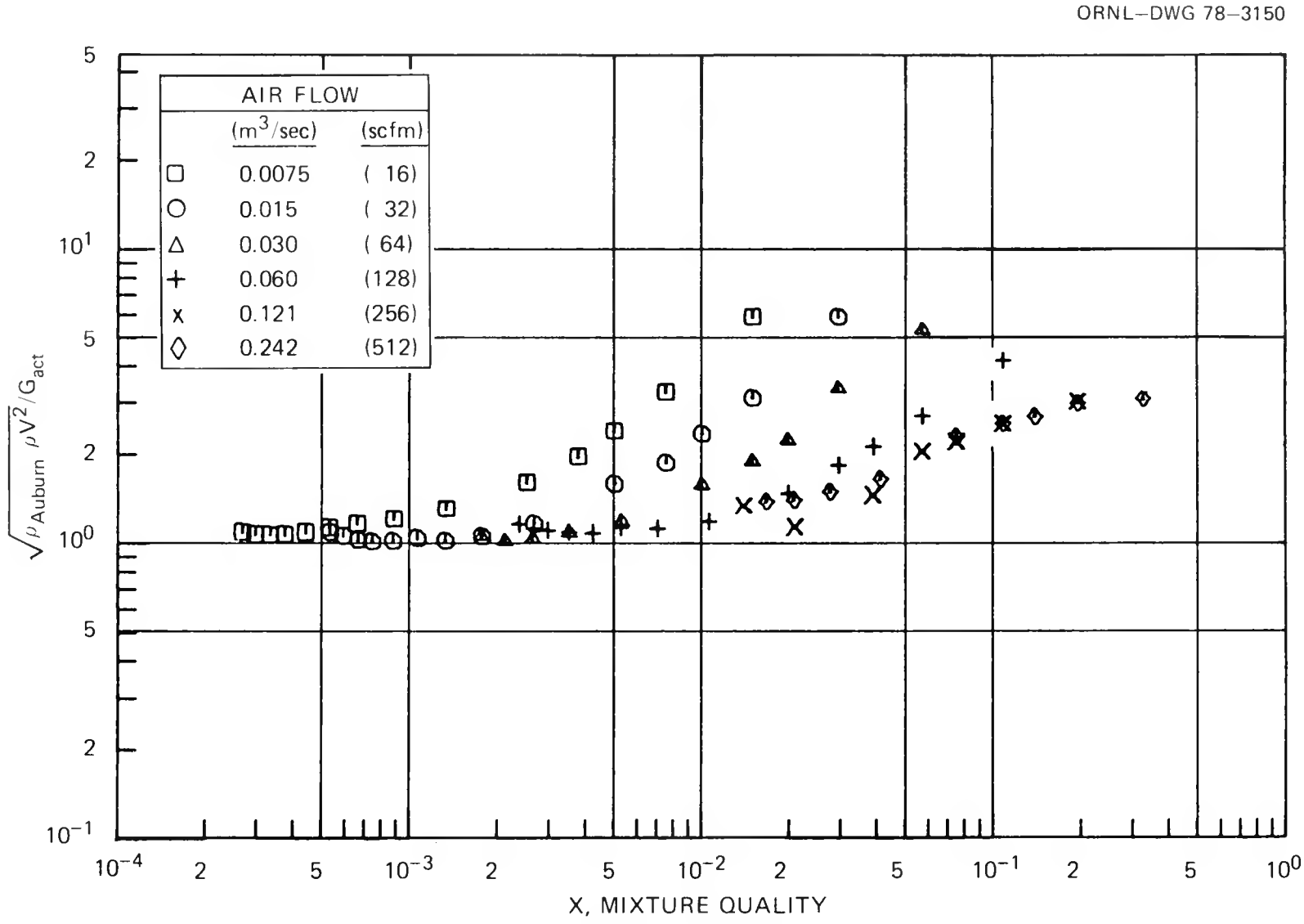

Fig. 4.12. Variation in the mass flow rate calculated using the one-velocity $G = \sqrt{\rho_{Auburn}\rho V^2}$ model as a function of mixture quality — no screens.

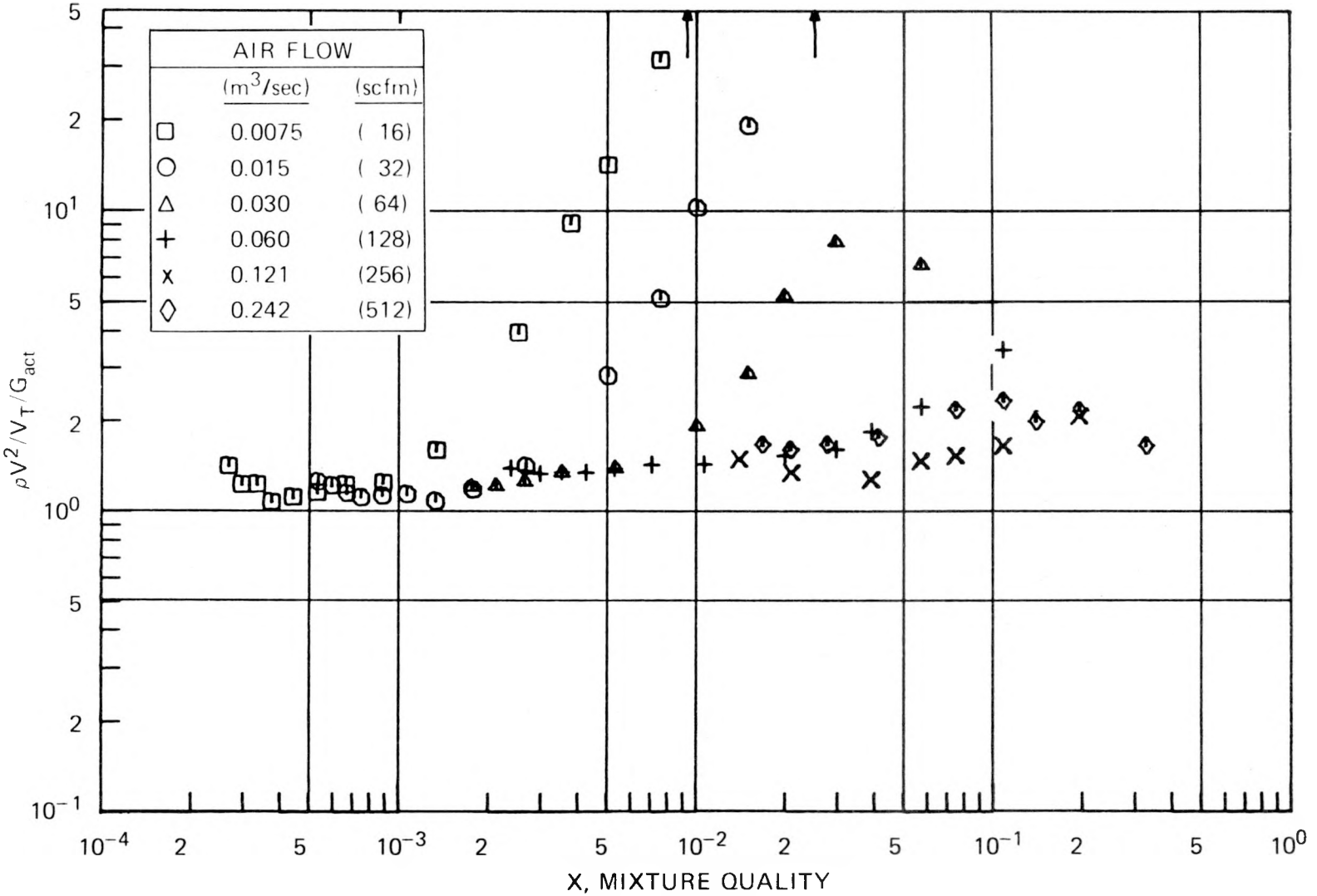

Fig. 4.13. Variation in the mass flow rate calculated using the one-velocity $G = \rho V^2/V_T$ model as a function of mixture quality — no screens.

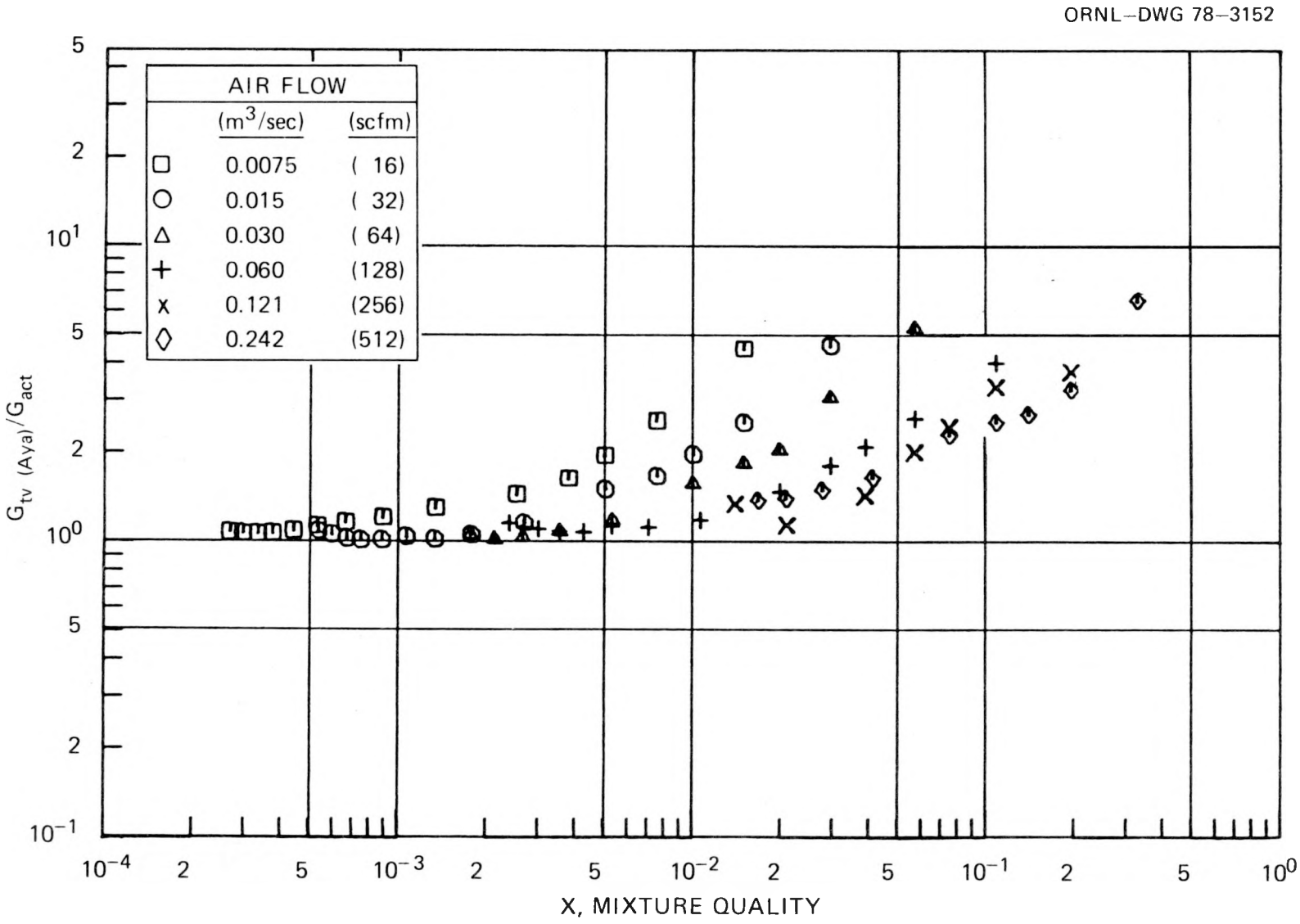

Fig. 4.14. Variation in the mass flow rate calculated using the two-velocity Aya model as a function of mixture quality — no screens.

reduction in the scatter has been achieved, although the results are not quite so satisfactory as those obtained by Sheppard et al.[6] with vertical downflow. Stratification effects in horizontal flow undoubtedly had some influence on these horizontal results since the greatest deviations occurred at the lowest flow rate where stratification can be expected according to the Baker[7] map.

The results from the tests using four 20-mesh screens to homogenize the flow are shown in Figs. 4.15 through 4.18. In Figs. 4.15 through 4.17, homogeneous flow is assumed. Comparing these to the corresponding Figs. 4.11 through 4.14 with no screens indicates that the 20-mesh screens reduce the scatter in the data. When the Aya model results of Fig. 4.18 are compared with those in Fig. 4.14, a small but definite decrease in the scatter can be attributed to the screens. Obviously, screens alone are not sufficient to homogenize the flow.

The effect of ramp orifices will be discussed in the next quarterly.

4.3 Auburn Meter Performance

J. E. Hardy P. A. Jallouk

In a previous quarterly report,[8] a comparison of the performance of the Auburn vapor fraction monitor with that of the three-beam gamma densitometer for vertical downflow was made. Generally, the two instruments showed reasonably good agreement up to a quality of 0.04, corresponding to a density of 0.05 g/cm^3 (3.7 lb_m/ft^3).

For the case of horizontal flow, a comparison of the Auburn-meter and gamma-densitometer-measured densities is shown in Figs. 4.19 and 4.20. As can be seen, both instruments agree very closely over the entire range of void fractions measured. The effect of the addition of the screens is shown in Figs. 4.21 and 4.22. A small decrease in the scatter of the data is noted.

The plots in Figs. 4.19 through 4.22 tend to magnify any differences between the two instruments in the high void fraction range and mask the differences at low void fractions. Consequently, Figs. 4.23 thrugh 4.26 were generated, and the void fraction results can be more meaningfully interpreted. The three-beam gamma densitometer and the Auburn meter seem

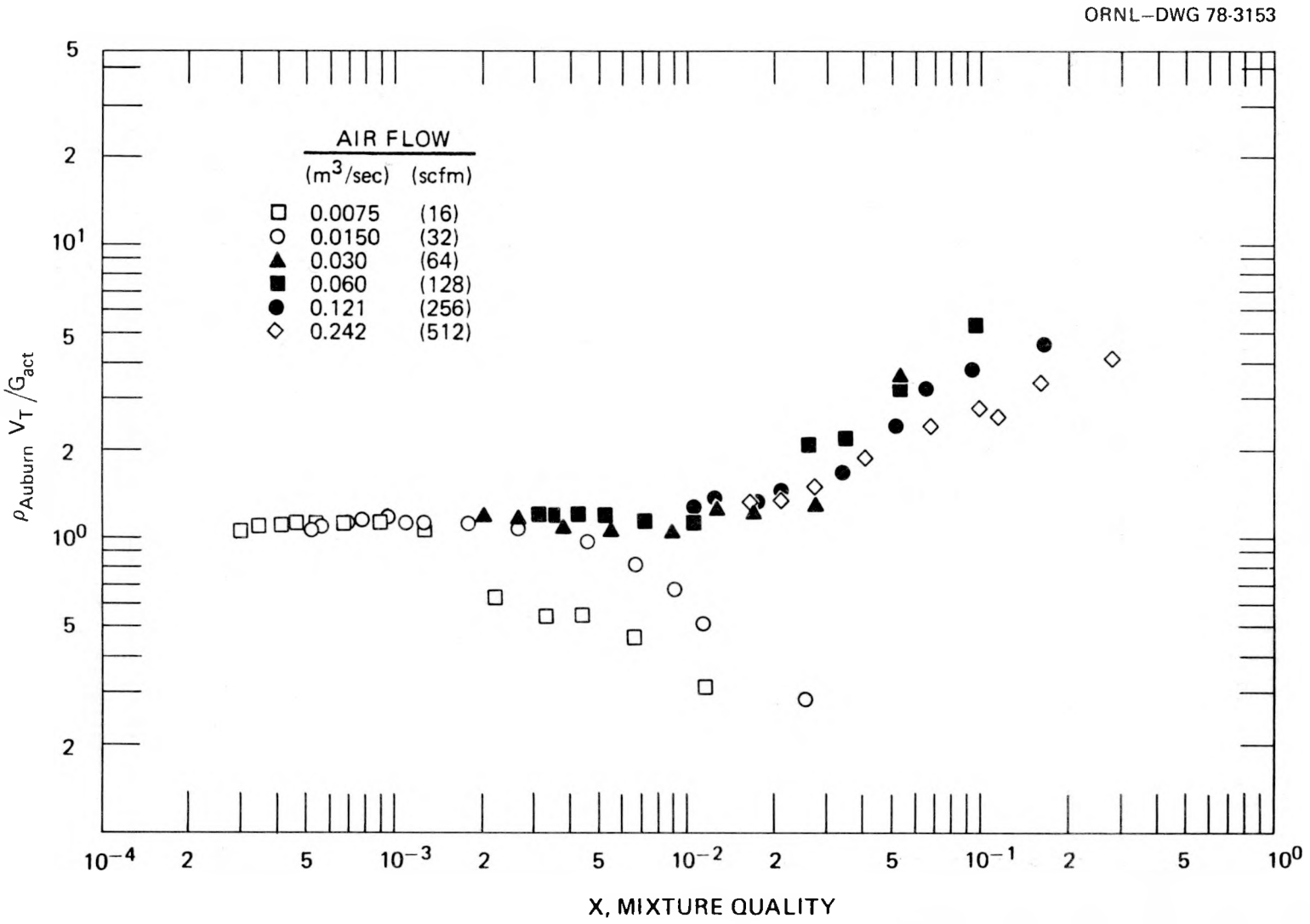

Fig. 4.15. Variation on the mass flow rate calculated using the one-velocity $G = \rho_{Auburn} V_T$ model as a function of mixture quality — four 20-mesh screens.

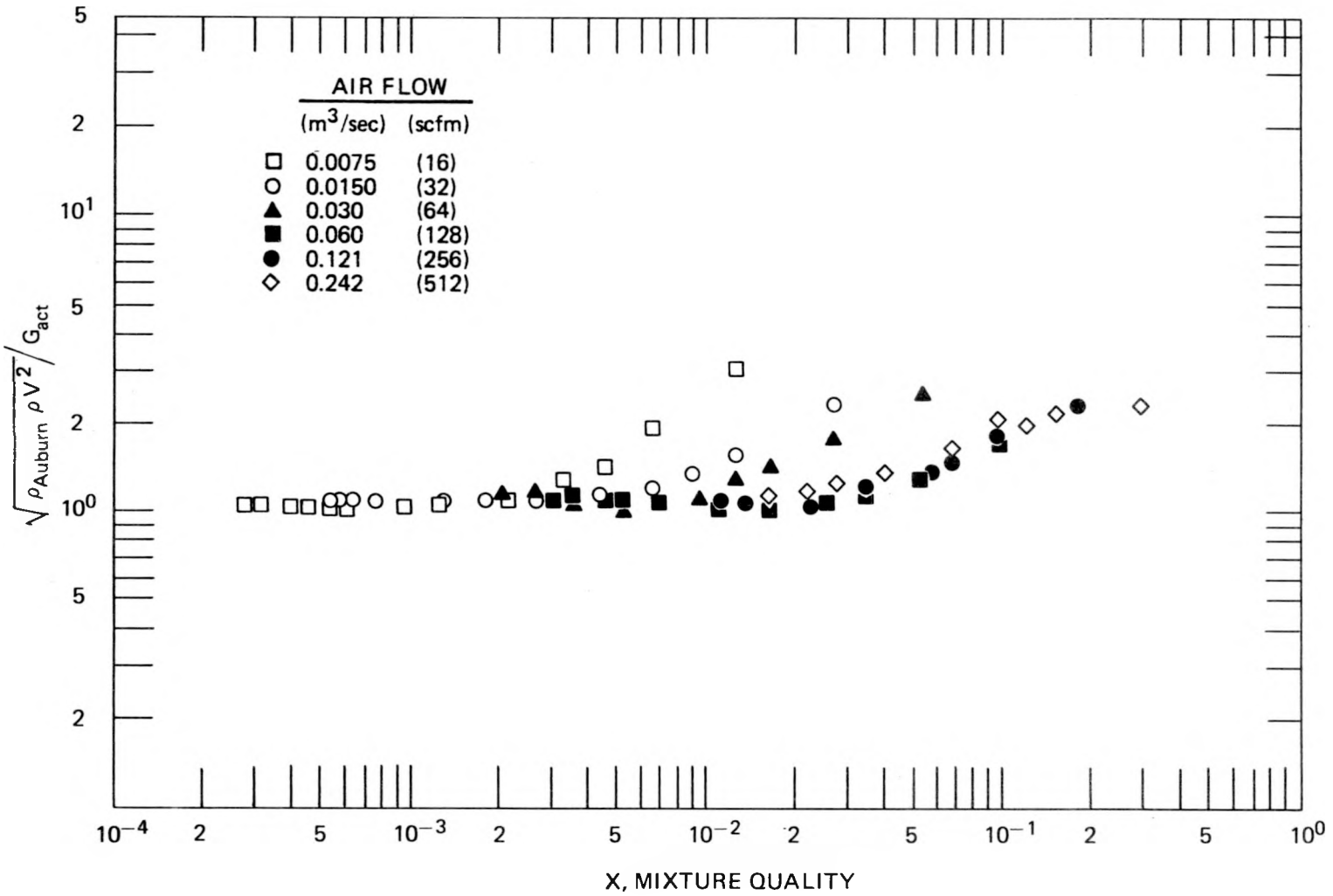

Fig. 4.16. Variation in the mass flow rate calculated using the one-velocity $G = \sqrt{\rho_{Auburn}\,\rho V^2}$ model as a function of mixture quality — four 20-mesh screens.

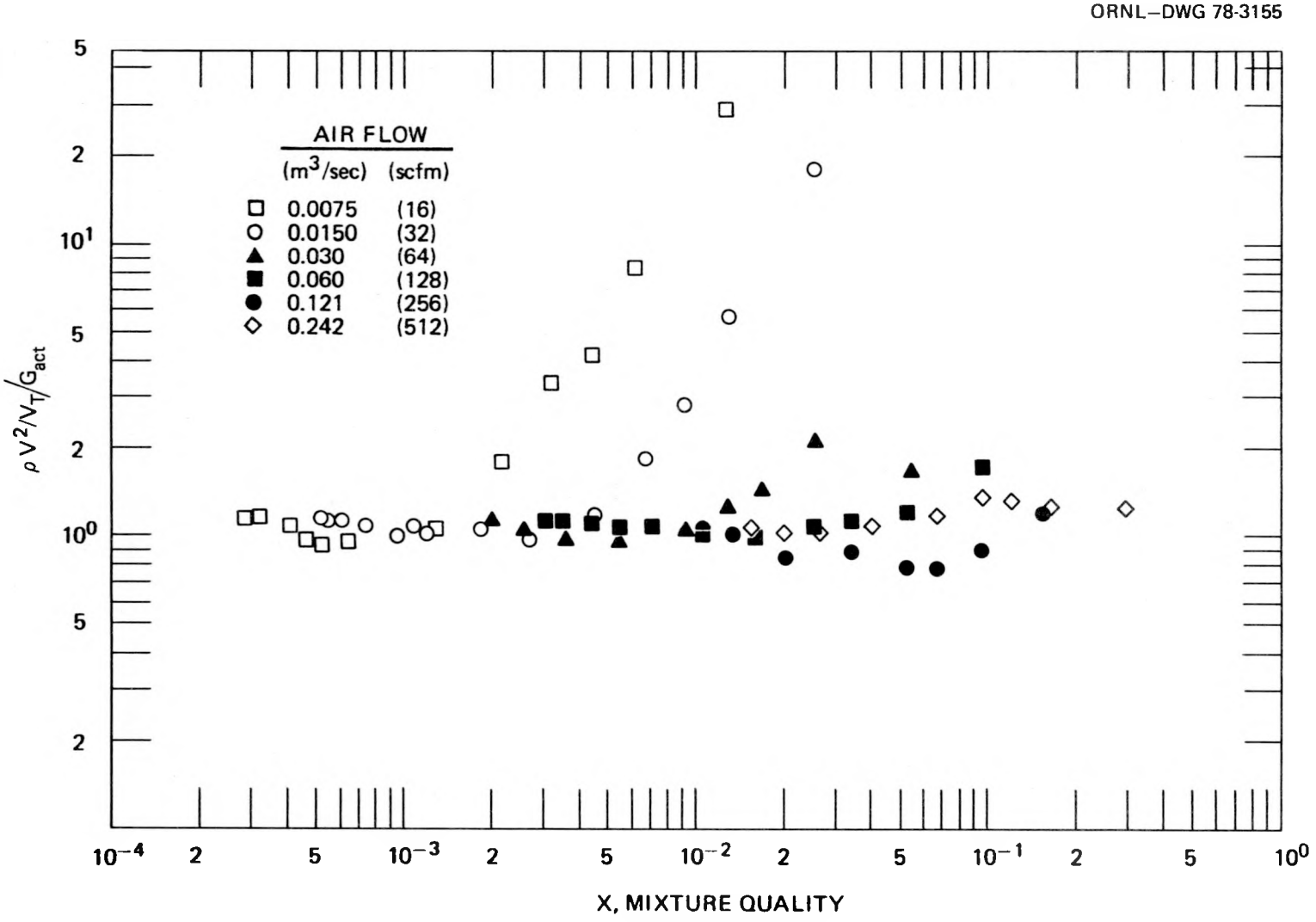

Fig. 4.17. Variation in the mass flow rate calculated using the one-velocity $G = \rho V^2/V_T$ model as a function of mixture quality — four 20-mesh screens.

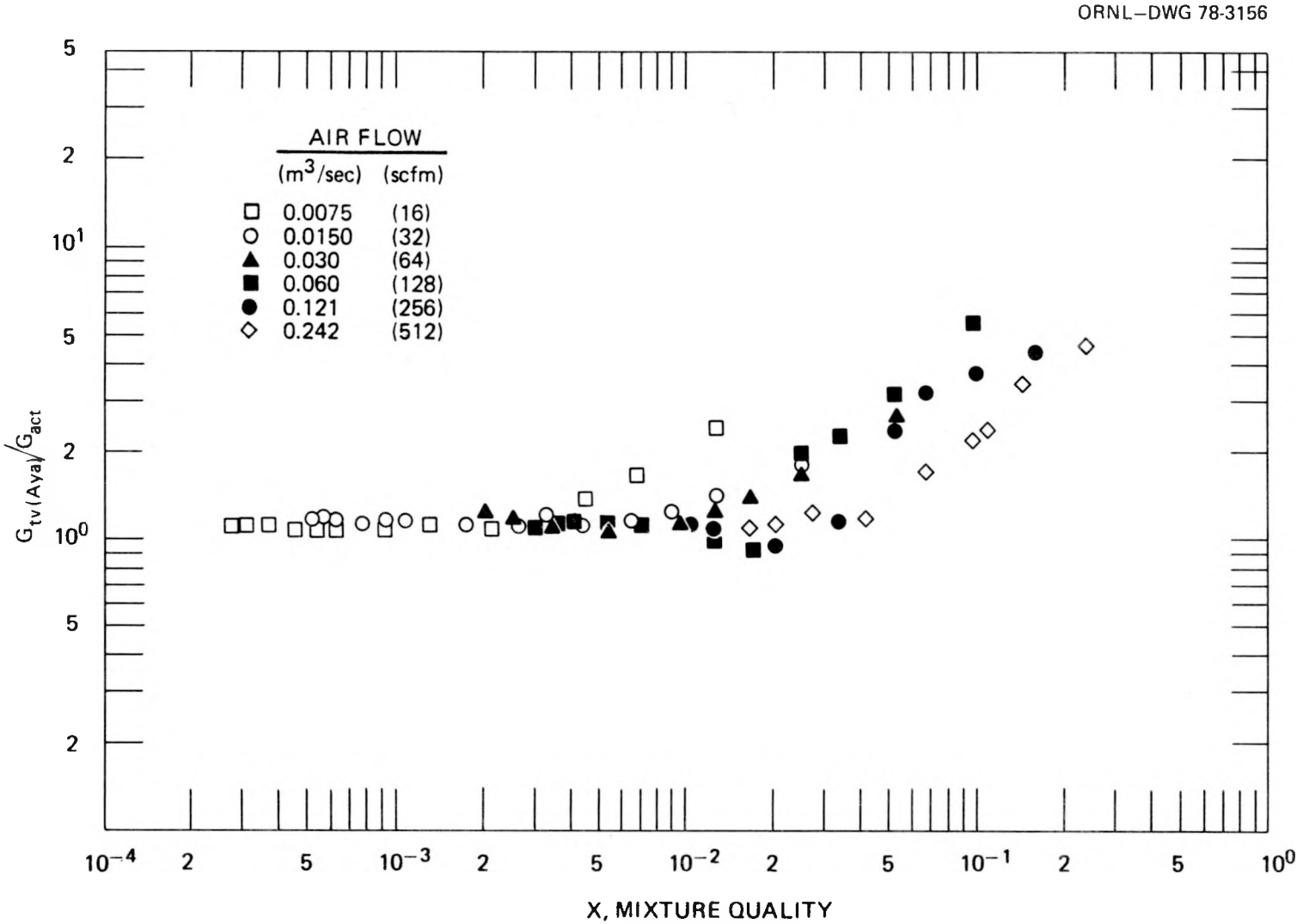

Fig. 4.18. Variation in the mass flow rate calculated using the two-velocity Aya model as a function of mixture quality — four 20-mesh screens.

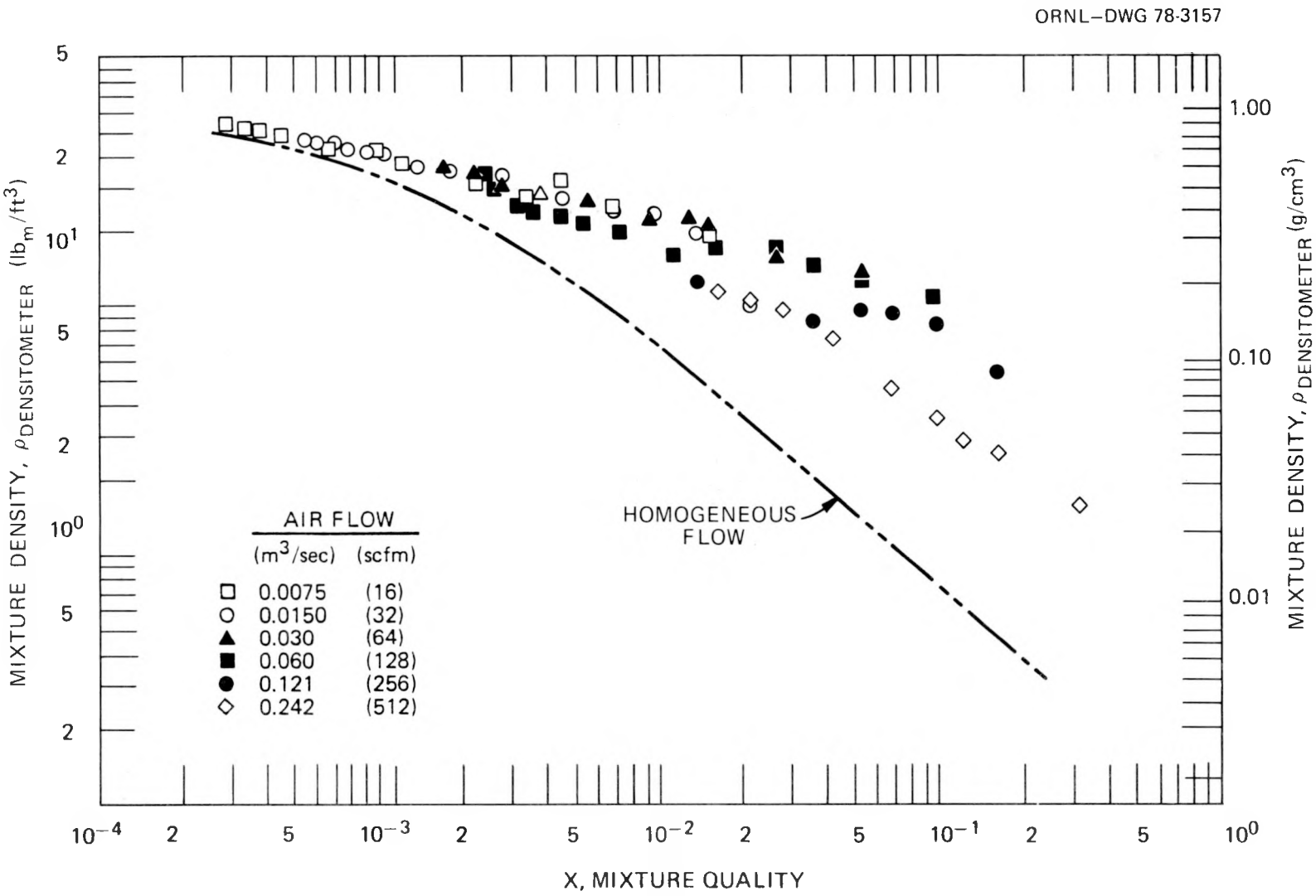

Fig. 4.19. Comparison of two-phase density given by three-beam gamma densitometer with the homogeneous flow model — no screens.

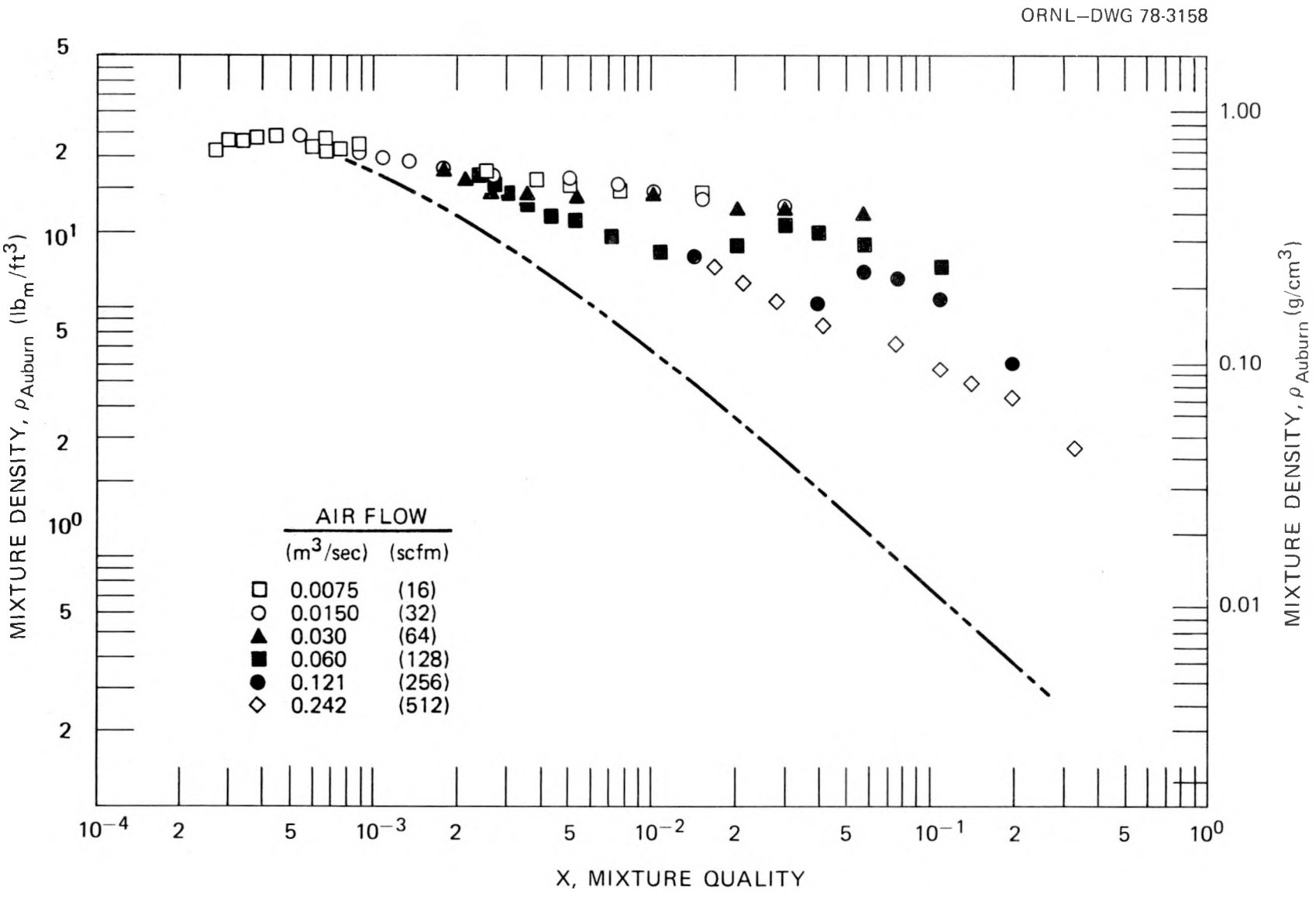

Fig. 4.20. Comparison of two-phase density given by Auburn meter with homogeneous flow model — no screens.

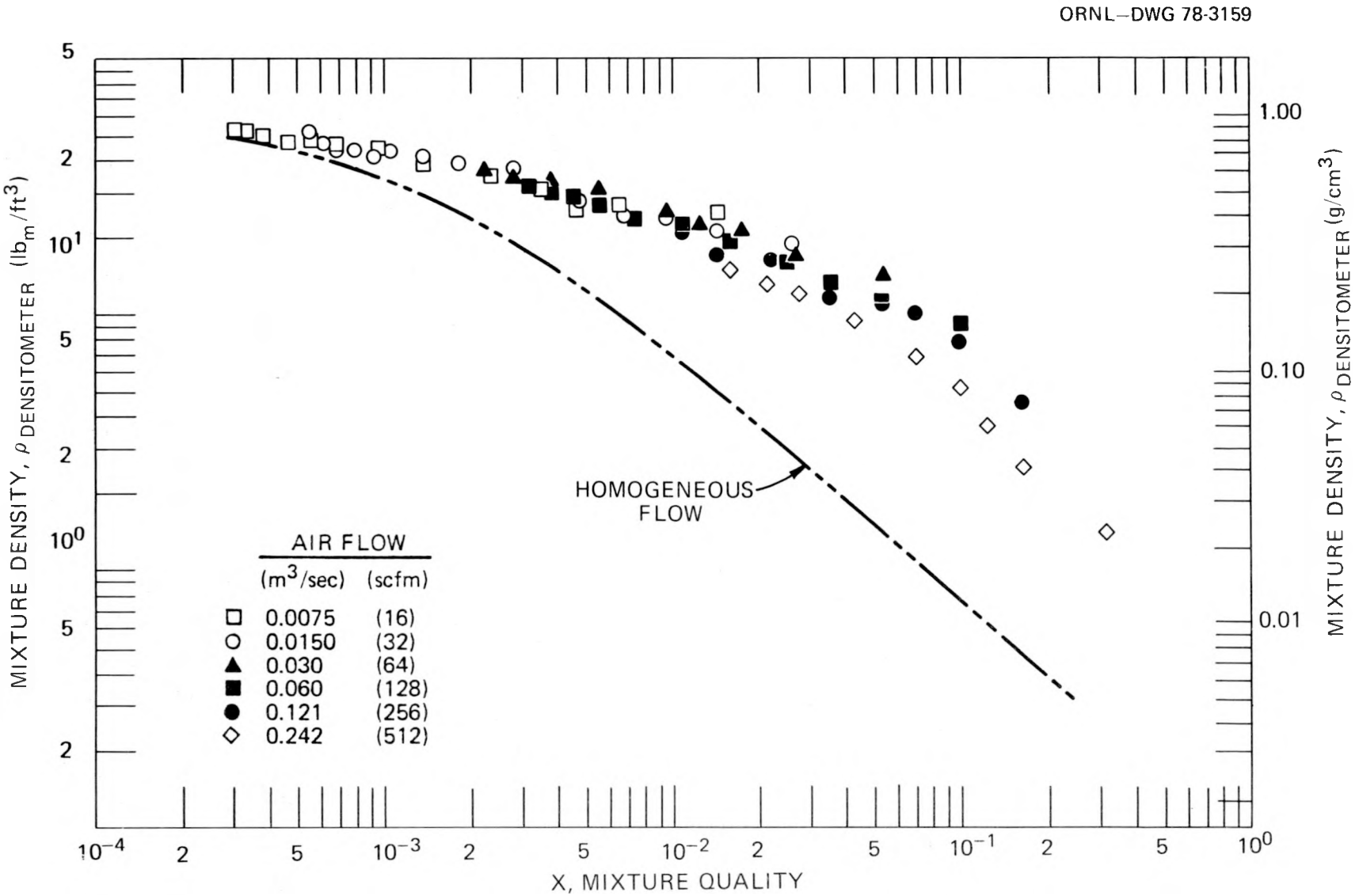

Fig. 4.21. Comparison of two-phase density given by three-beam gamma densitometer with homogeneous flow model — four 20-mesh screens.

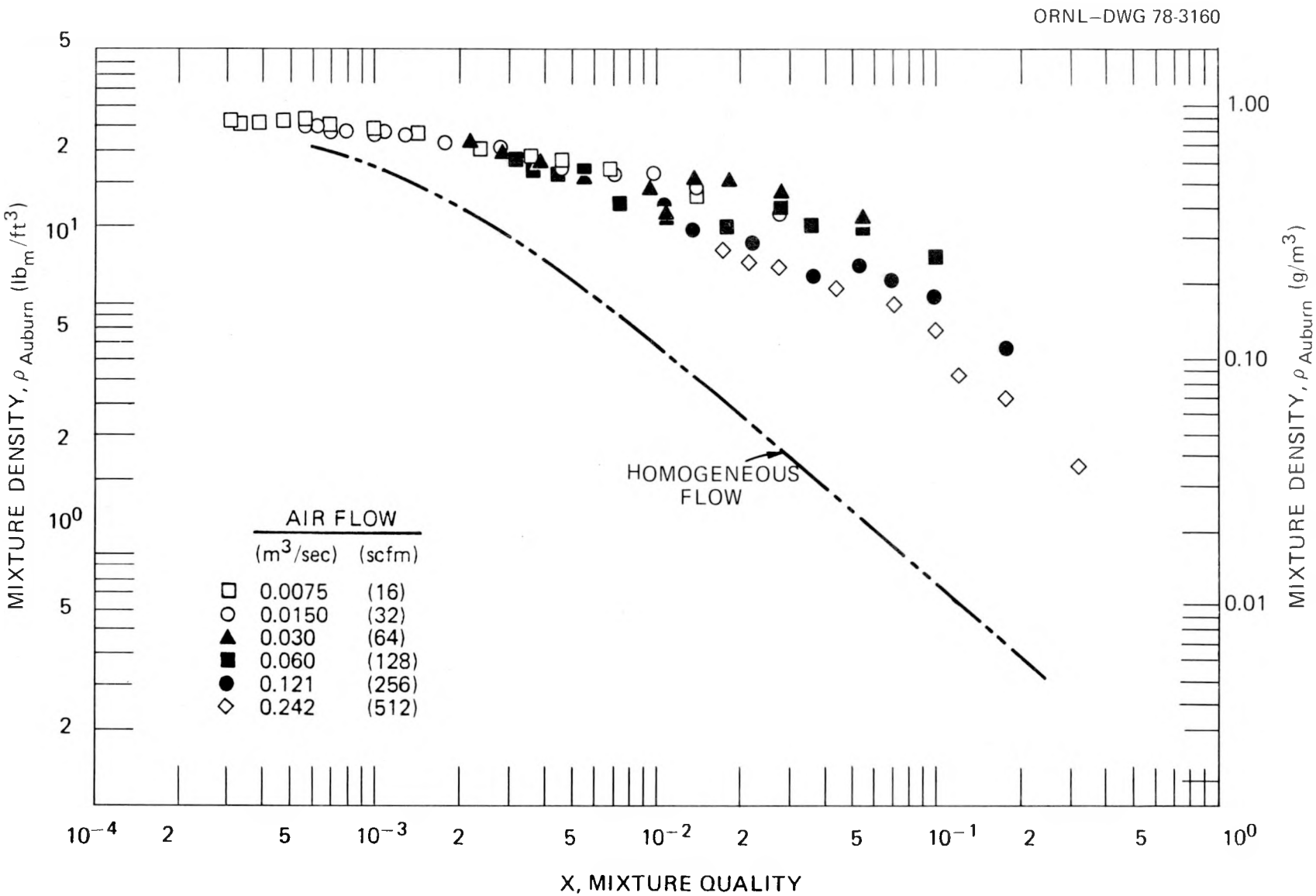

Fig. 4.22. Comparison of two-phase density given by Auburn meter with homogeneous flow model — four 20-mesh screens.

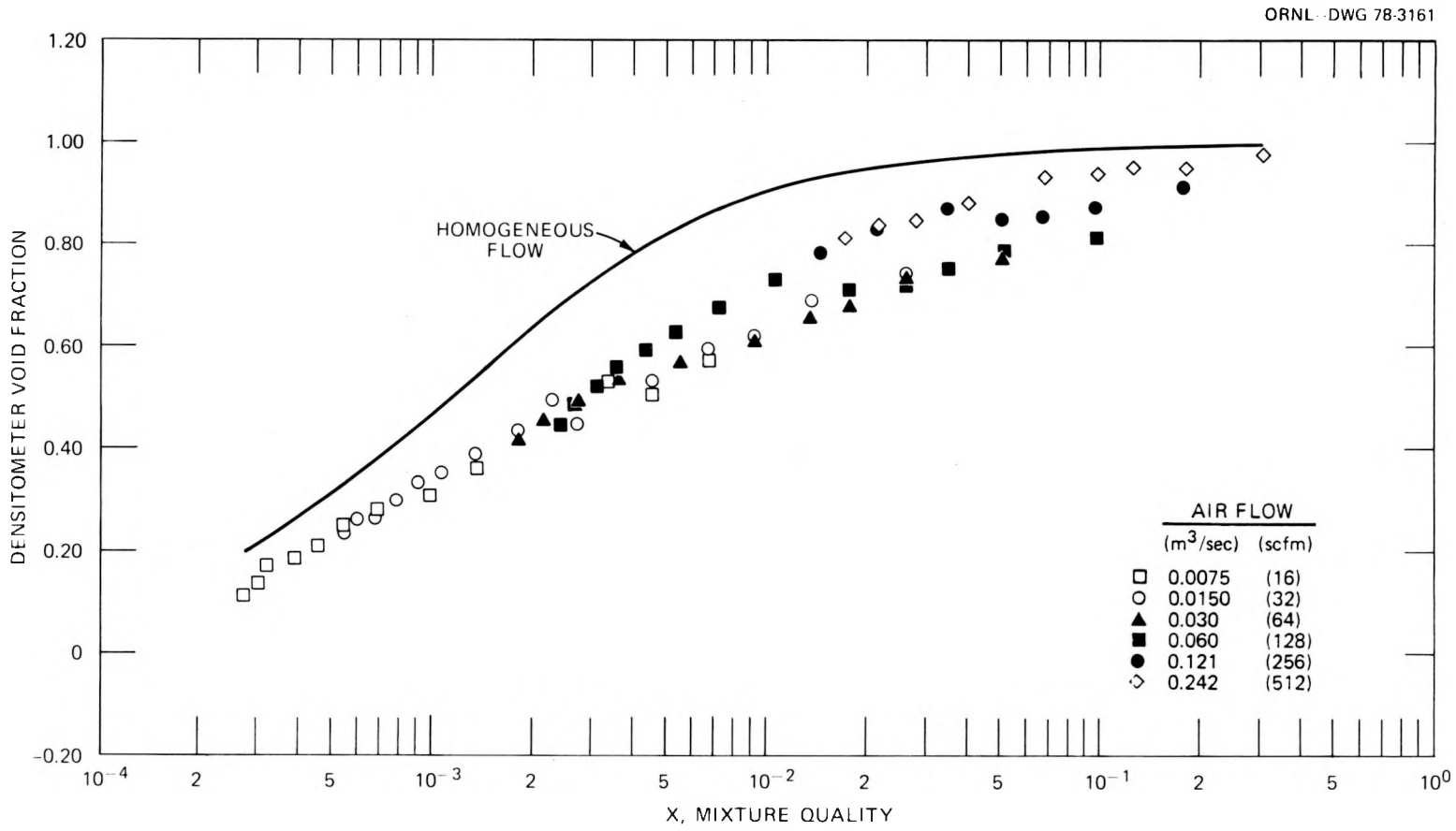

Fig. 4.23. Comparison of the composite void fraction given by the three-beam gamma densitometer with the homogeneous flow model — no screens.

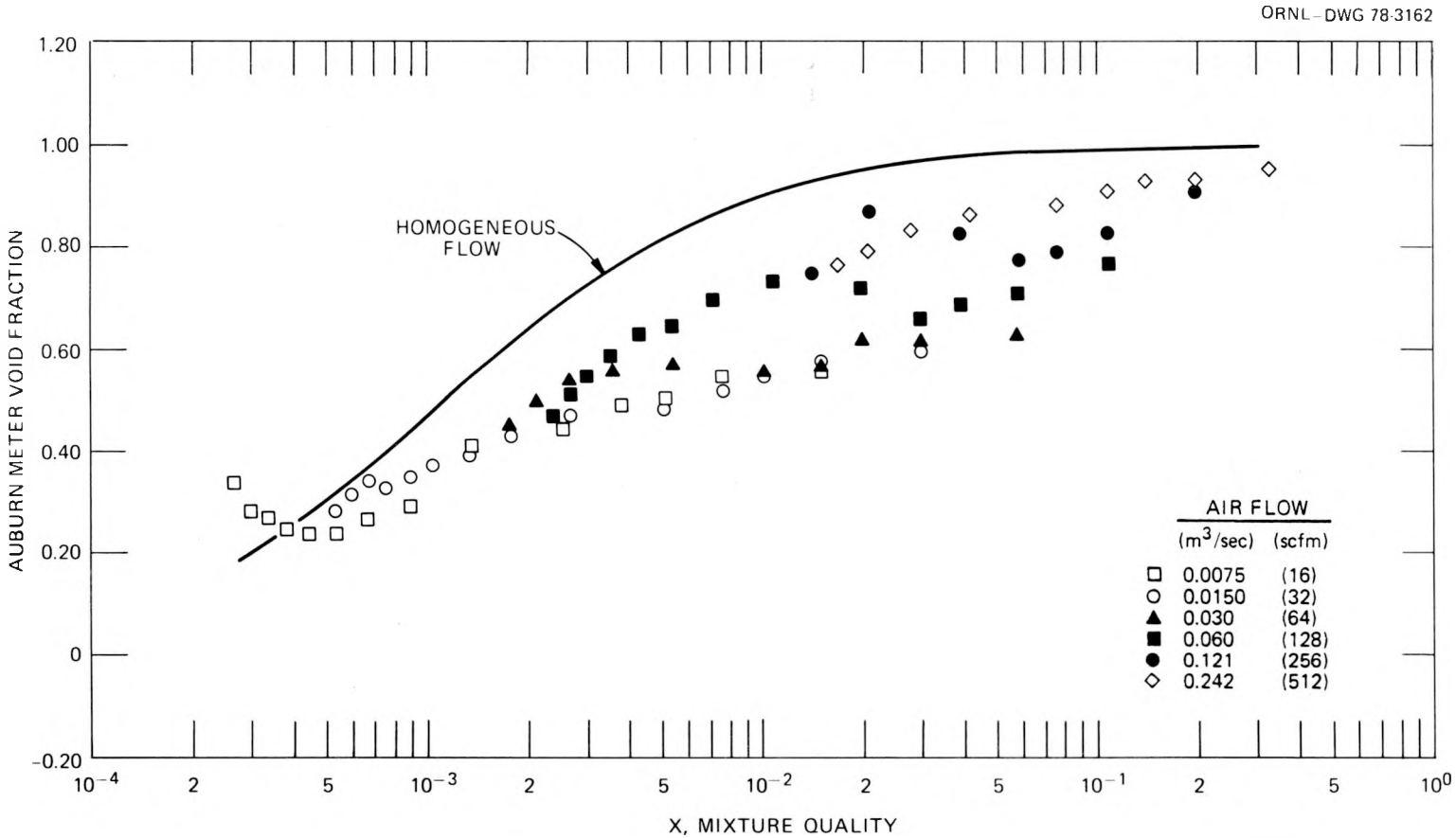

Fig. 4.24. Comparison of Auburn meter void fraction with the homogeneous flow model — no screens.

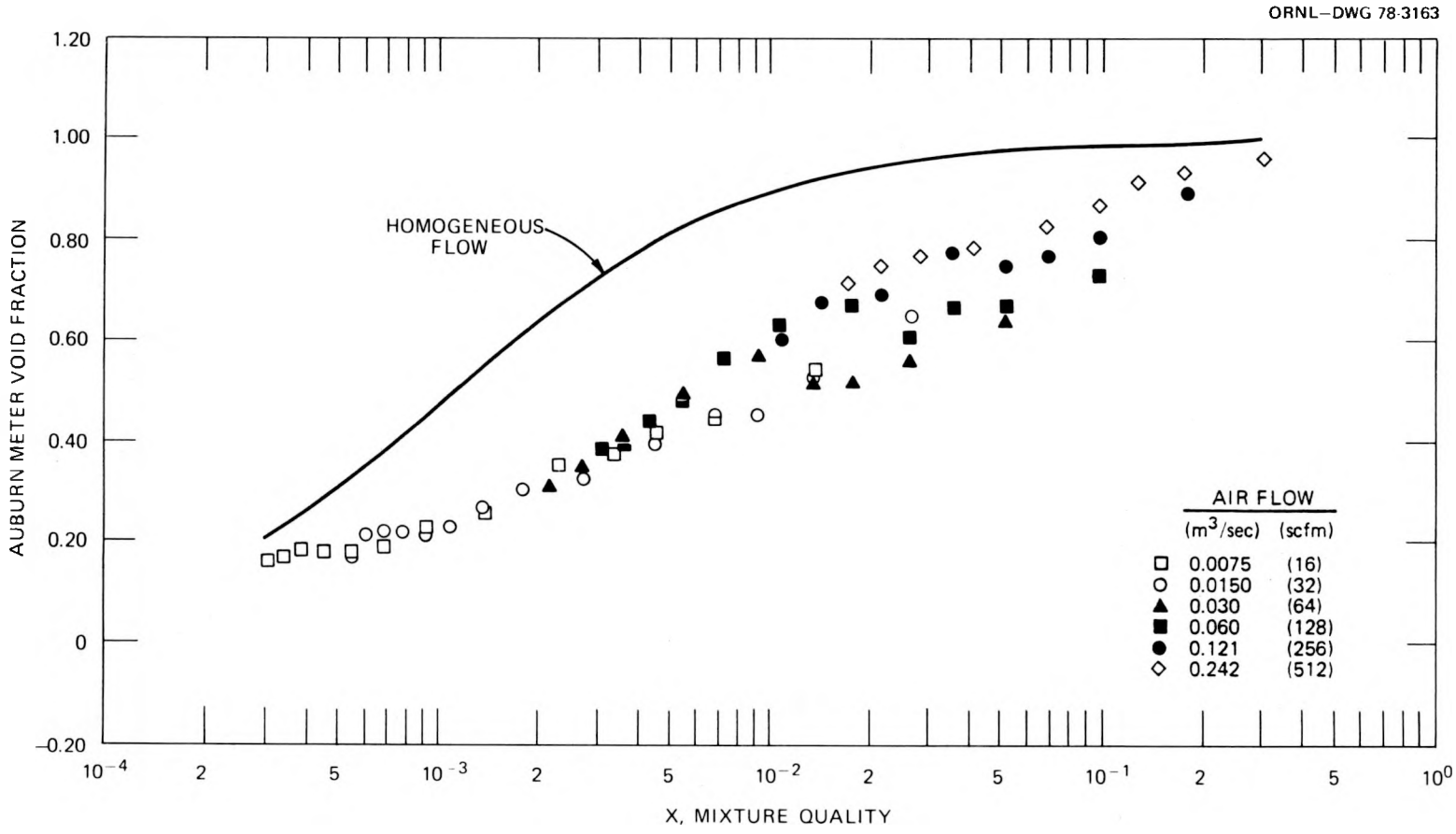

Fig. 4.25. Comparison of the composite void fraction given by the three-beam gamma densitometer with the homogeneous flow model — four 20-mesh screens.

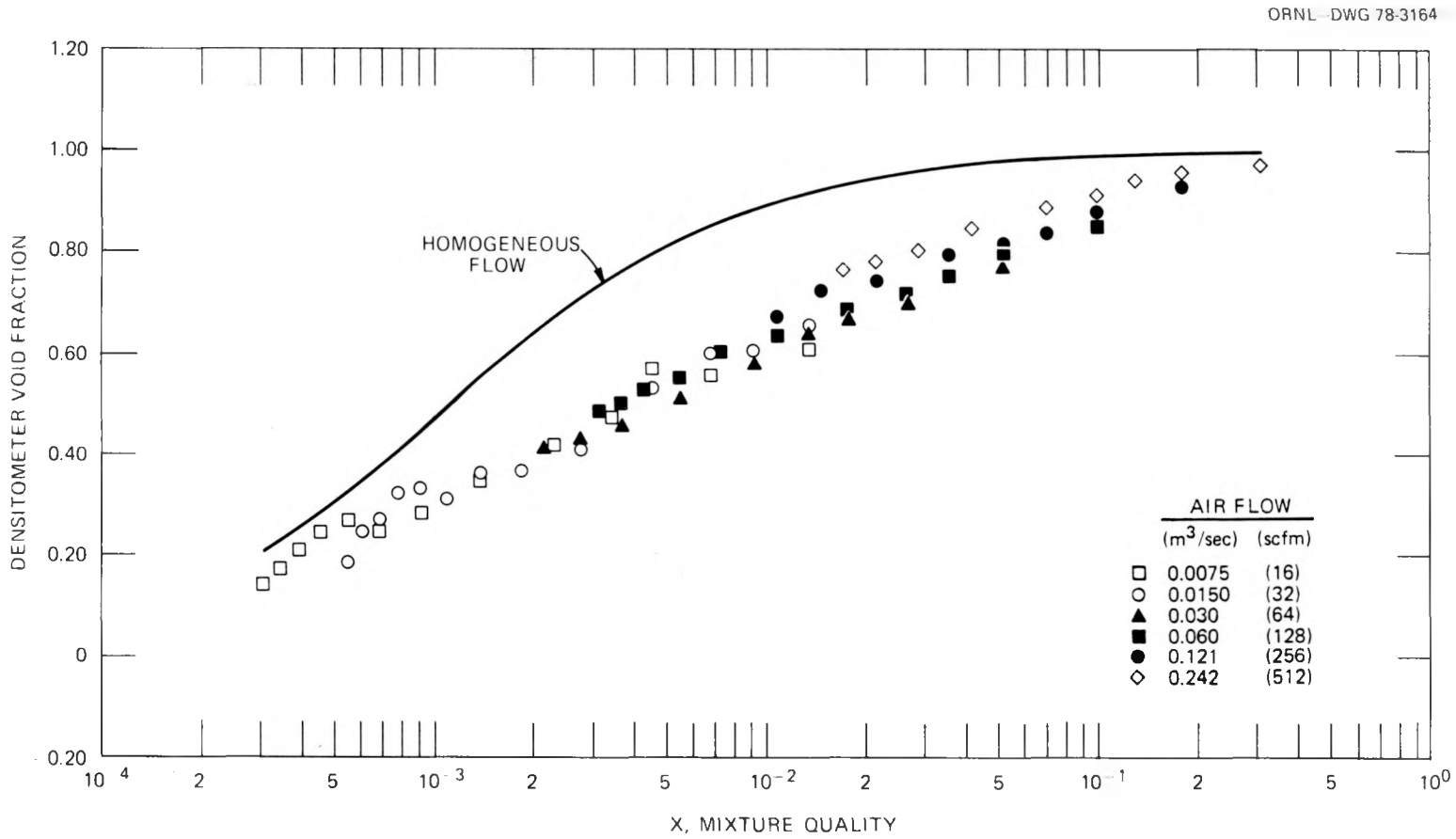

Fig. 4.26. Comparison of Auburn meter void fraction with the homogeneous flow model — four 20-mesh screens.

to agree with each other over the entire void fraction range. The scatter in the data was, however, larger with the Auburn meter, indicating the possibility that the Auburn meter is more flow regime dependent than the three-beam densitometer.

Thus, for vertical downflow and horizontal flow, the Auburn meter can be a less expensive substitute for a gamma densitometer in the range of parameters tested here if the limitations of the meter are understood.

5. THERMAL-HYDRAULIC TEST FACILITY INSTRUMENTATION

A. F. Johnson* R. C. Muller*
B. J. Veazie* W. R. Miller*

5.1 Instrumentation Design in Progress

Design is in progress on several upgrades, modifications, and additions to the instrumentation of the THTF.

The turbine meter electronics which converts the frequency and phase of two pickoff probes to an analog indication of flow is being redesigned. The frequency response of the present electronics from Flow Technology, Inc., is too slow to follow the initial blowdown transient. The redesigned electronics measures the period of each cycle of the probe output, inverts the period to obtain frequency, and provides a bipolar analog output as an indication of the flow. With the redesigned electronics, the limitation on frequency response will essentially be that of the turbine itself (∿15 msec time constant). A prototype of the redesigned electronics has been built and tested in the laboratory and, in parallel with the existing electronics, has been through one blowdown test. Fabrication has begun on the production units, and installation is scheduled for early in the bundle 2 test series.

Several design changes are necessary to accommodate the additional instrumentation for bundle 2. Four heater rods will be built incorporating Chromel/Constantan, Nisil/Nicrosil, and Copper/Constantan sheath thermocouples in addition to the standard Chromel-Alumel thermocouples. Additional compatible extension wire and patch panel plugs are being provided to handle the alternate thermocouple types. Bundle 2 will also contain one liquid-level probe built by EG&G Idaho. Space and cabling for the signal conditioning are being provided as well as the interconnection with the data acquisition system. These items will be completed prior to the installation of bundle 2.

A conceptual design for an automated calibration and verification system for the THTF instrumentation is underway. The system is to permit

---

*Instrumentation and Controls Division.

channel-by-channel calibration and checkout of the data acquisition system. Additionally, the system will permit functional verification of critical field instrument loops, for example, by measuring center thermocouple insulation resistance and by shunt calibration of strain-gage bridge transducers. The conceptual design and cost estimate are scheduled to be completed in the first quarter of CY 1978.

Design is in progress for additional transient instrumentation spool pieces in the THTF. The locations of the additional spool pieces are the pressurizer outlet leg, the pump bypass line, and the primary outlet lines (3) of the main heat exchangers. Installation is scheduled to be completed prior to bundle 3 but depends somewhat on the schedule for piping modifications.

Design is nearing completion on equipment and wireway layouts and clean electrical power wiring for the auxiliary control room. This room will house the upgraded data acquisition system and the signal conditioning equipment for bundle 3, and beyond, instrumentation. Initial occupancy should be in the first quarter of CY 1978.

5.2 Instrumentation Evaluation and Analysis in Progress

The ongoing effort to evaluate and analyze the performance of the THTF instrumentation is presently concentrated on two types of transient instrumentation: drag disks and differential pressure transducers. The main thrust of the present activity is to characterize the effects of various parameters on the existing instruments so that existing data can be corrected by taking these effects into account and to establish error bands for these measurements. Recommendations can then be made for improving the instruments in the future.

The drag disks are presently being studied to characterize the effects of temperature on measurement in an effort to reduce the error bands on the steady-state readings. This effort consists of examining a large volume of flow calibration data taken in the THTF as well as a series of out-of-loop tests utilizing temperature-controlled ovens.

The differential pressure measurement system is being studied to derive a transfer function so that the actual hydraulic phenomena of

interest during a transient can be "backed out" of the data in the presence of substantial "ringing" in the signal. Included in the investigation is the construction of a small pipe section which can be subjected to a pressure impulse via a hydraulic cylinder. With this test rig, the effects of length and complexity in tubing runs can be evaluated. Various transducers and transducer configurations can also be easily evaluated.

Evaluation of instruments for bundles 2 and 3 is also in progress. As reported elsewhere in this report, the liquid-level measurement system procured from EG&G Idaho for use in bundle 2 has been subjected to several tests in the FCTF to evaluate its performance. More subchannel bulk fluid temperature measurements within the heater bundle are also desired. Therefore, the installation of thermocouples on several of the grid spacers in order to measure the transient temperature of the bulk fluid is being studied. Tests will be run in the bundle hydraulics test stand to determine the effects, if any, of these thermocouples on pressure drop and mixing at the grid spacers. The best method of attachment and configuration will then be determined and incorporated into the bundle 3 design.

6. BUNDLE 2 FUEL PIN SIMULATORS

A. N. Smith R. L. Ludwig*
W. E. Baucum R. W. McCulloch

As reported previously, some of the bundle 2 fuel pin simulators are somewhat longer than the specified length and cause the sheath thermocouples to exit the unit at a point higher in the bundle assembly than was designed. The exit point of the thermocouples from the heater can be lowered by trimming back the upper part of the outer sheath to a point near the beginning of the seal-bearing oversleeve. While performing this trimming operation, a crack was discovered in the inner sheath just above the seal-bearing oversleeve. To investigate this situation, this unit (serial No. 1U91) was subjected to destructive analysis. The outer sheath was removed along its entire length to look for other cracks, and cross sections were cut and examined at crack locations.

Many other cracks were found after removal of the outer sheath; in fact, 70% of the length of one entire groove was found to be cracked. Cracks were found only in the bottom of the inner sheath grooves which carry the sheath thermocouples. A typical crack is shown in Fig. 6.1. Figure 6.2, a cross section of this area, indicates that a single groove actually consists of two subgrooves, each designed to carry one thermocouple. Figures 6.3 through 6.6 show each of the four grooves at a higher magnification. There is a through crack in subgroove 2 of groove 1, and incipient cracks are seen in both subgrooves of groove 4. There is also evidence of small incipient cracks in subgroove 2 of both grooves 2 and 3. Subgroove 2 was machined deeper than subgroove 1 in every groove, and the minimum metal thickness at the bottom of subgroove 2 was about 0.018 cm (0.007 in.). For groove 1, subgroove 1 was found to be cracked over approximately 6% of its length, whereas subgroove 2 was cracked over 71%. Figure 6.7 shows the outer sheath in the area of a thermocouple groove after it had been removed from the inner sheath. The thickening of the outer sheath, which took place only over the area of the thermocouple

*Y-12 Development Division.

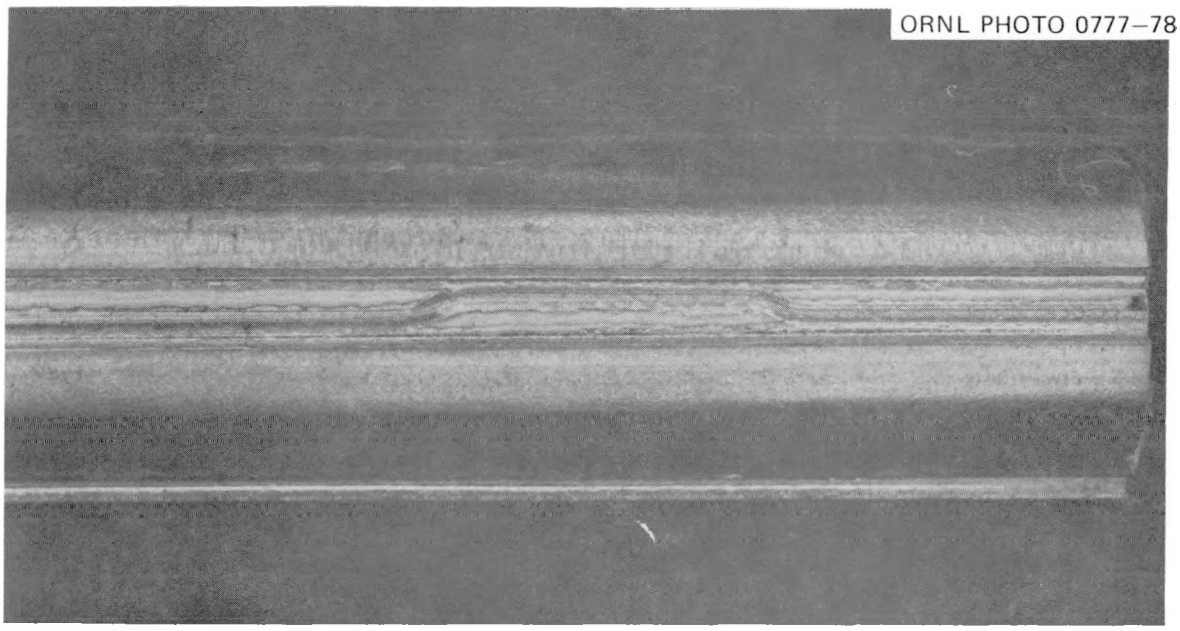

Fig. 6.1. Through crack in groove 1 about 35 cm from lead end of heater (5×).

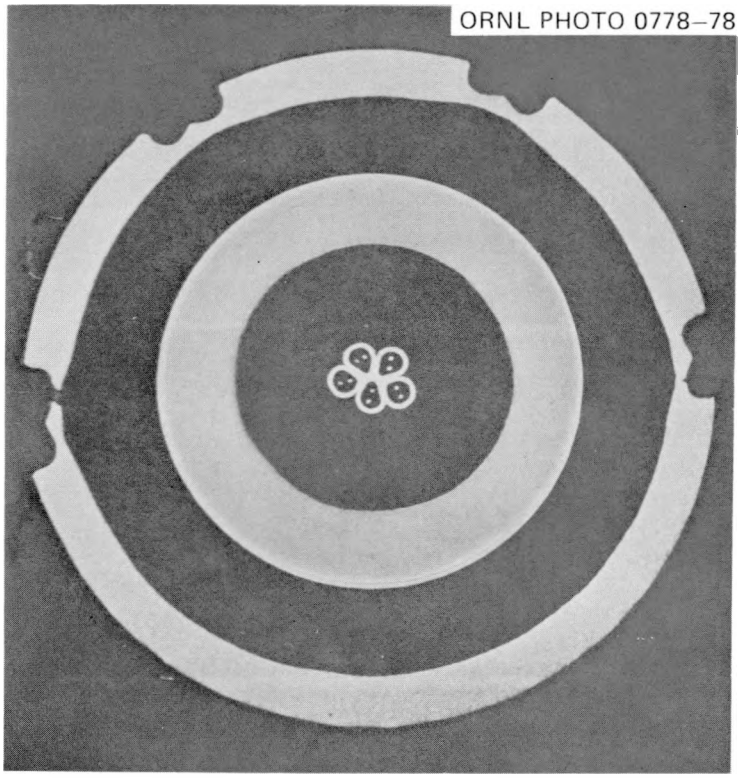

Fig. 6.2. Section of heater 36.8 cm from lead end. Section taken facing ground plug end. In all grooves, subgroove 1 is on the left and subgroove 2 on the right (8.5×).

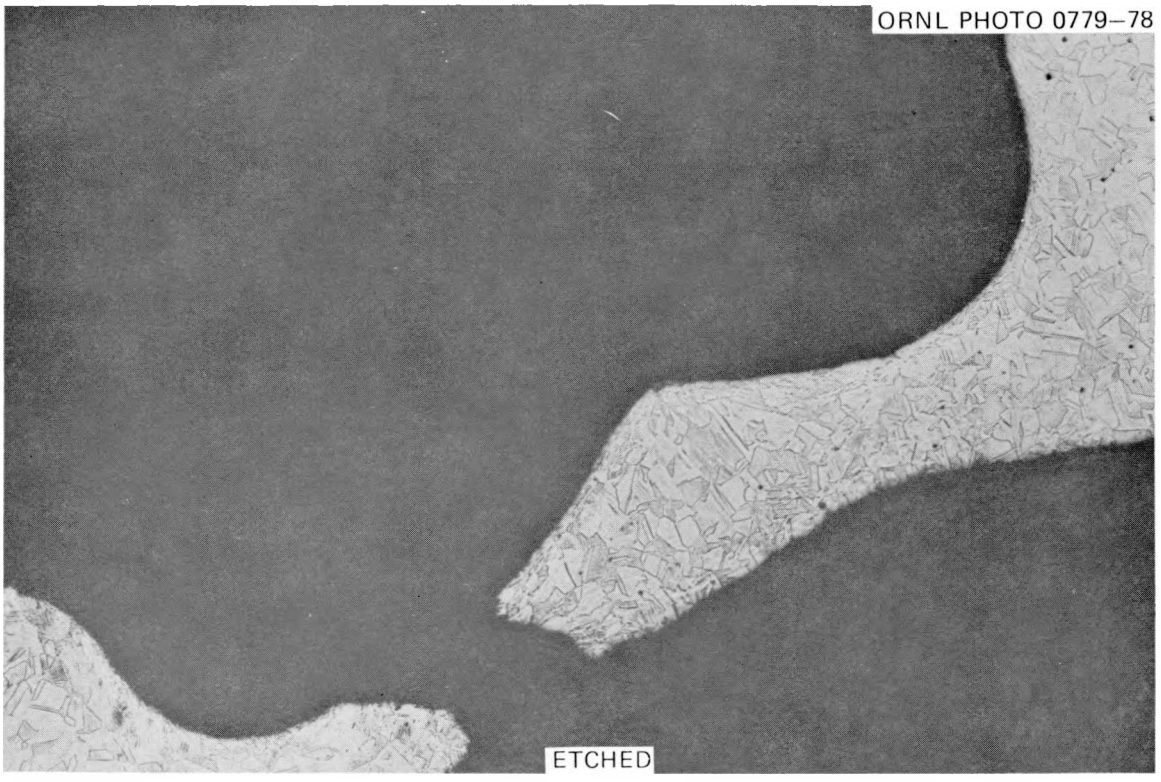

Fig. 6.3. Groove 1, section 36.8 cm from lead end of heater. Subgroove 2 (left) shows crack (100×).

groove in the inner sheath, indicates that the thermocouple did not fill up the groove in the inner sheath before swaging so that during swaging the outer sheath thickened to fill the remaining volume.

The inner sheath cracks apparently occurred during the process of swaging on the outer sheath since the manufacturer indicated that the grooves were not machined until after the inner sheath had been swaged. This is a very light swaging process with the outer diameter of the inner sheath reduced by only 0.0254 cm (0.0100 in.), but apparently the pressure on the bottom of the groove was sufficient to cause the initiation of cracks. Our analysis has shown that the groove was machined somewhat deeper than was necessary so that the metal thickness at the bottom of the groove was on the order of 0.0178 cm (0.007 in.). Also, one subgroove was machined deeper than the other, and that subgroove showed a greater tendency to crack. This evidence suggests that the major cause of the cracking was the improper machining of the grooves in the inner sheath.

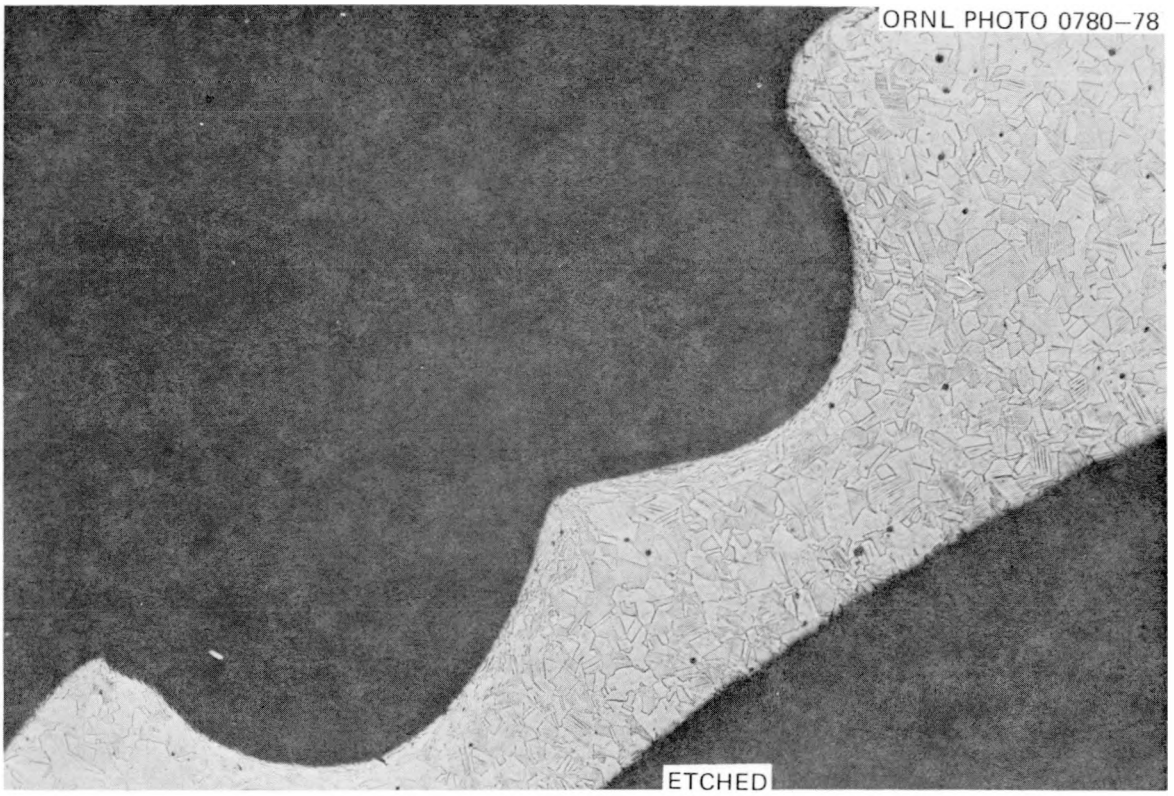

Fig. 6.4. Groove 2 section 36.8 cm from lead end of heater. Subgroove 2 on left (100×).

Another factor to be considered is the density of the boron nitride (BN) insulation inside the inner sheath. The density of the BN insulation would act to resist the reduction of diameter in the sheath and would thus affect the pressure on the inside surface of the inner sheath groove. Somewhat greater BN density would be expected in bundle 2 than in bundle 1 because the outer sheath for bundle 2 is 0.0127 cm (0.005 in.) thicker than that for bundle 1 while the outside diameter of the finished fuel pin simulator is the same. This means that the outside diameter of the BN layer was compacted to a diameter 0.0127 cm (0.005 in.) smaller, and thus it would be expected to have a higher density. Also, inspection records show that in some of the bundle 2 fuel pin simulators, including this one analyzed, the fill weight of the BN was somewhat higher than the weight that would normally be expected, a condition which would increase the BN density. It is likely that this density effect also played a significant role in the formation of cracks.

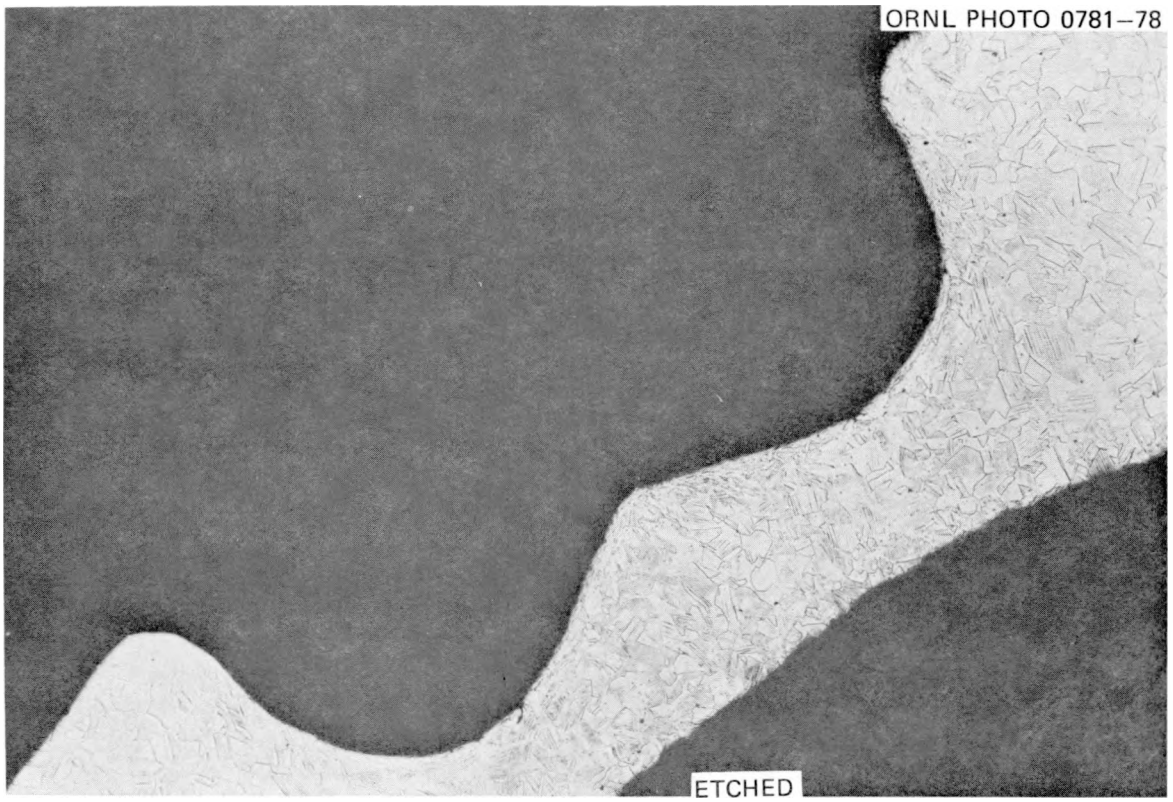

Fig. 6.5. Groove 3 section 36.8 cm from lead end of heater. Subgroove 2 on left (100×).

The effects of these cracks on the operational life and performance of the fuel pin simulator is still somewhat unknown. It has been hypothesized that since the liquid and pressure barrier is actually the outer sheath [which is 0.0127 cm (0.005 in.) thicker than for bundle 1 fuel pin simulators], the presence of cracks would not be detrimental to the operation of the bundle 2 fuel pin simulators. This has been partially substantiated by the examination of a bundle 2 fuel pin simulator which had been severely operated in the FCTF and had shown satisfactory performance. Examination showed that the inner sheath of this unit was also cracked in one area. However, the extent of cracking in this unit was much less than in the unit examined previously, and it is possible that the sheath was not initially cracked but was cracked during operation. It may be necessary to operate other bundle 2 fuel pin simulators which are known to have cracked sheaths in the FCTF to obtain better statistical data.

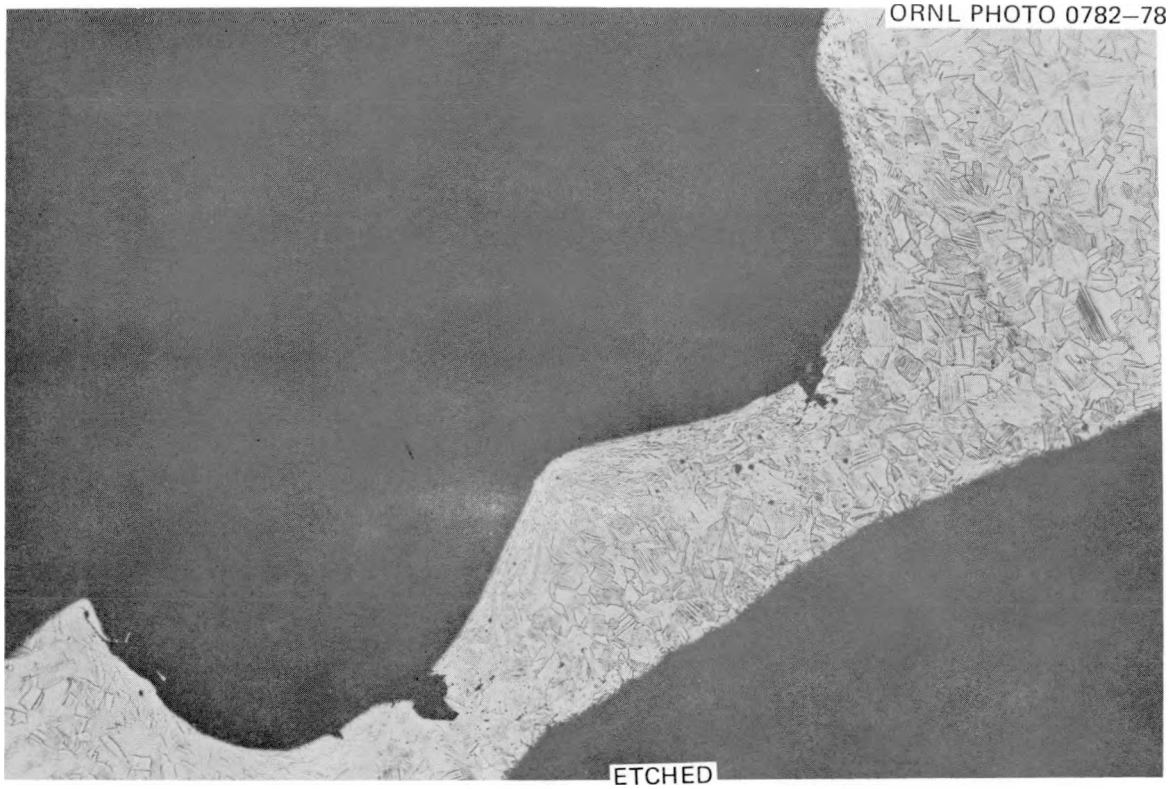

Fig. 6.6. Groove 4 section 36.8 cm from lead end of heater. Subgroove 2 on left (100×).

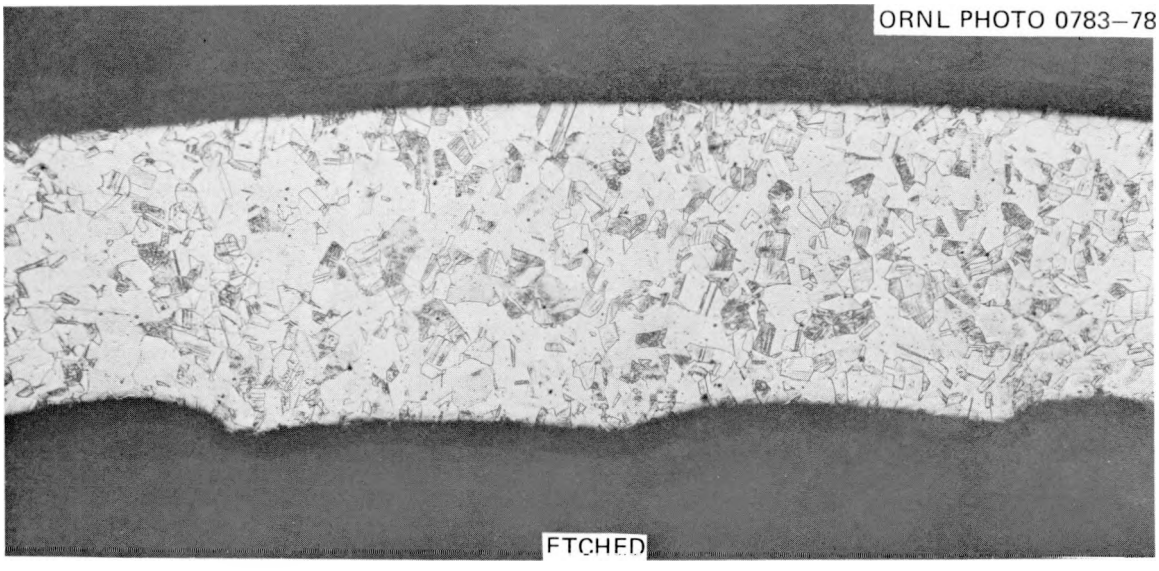

Fig. 6.7. Section of outer sheath over groove 1, 218.6 cm from lead end of heater (100×).

It is not known at this time how many of the bundle 2 fuel pin simulators have cracks in the inner sheaths; cracks have been found in at least two other simulators while trimming back the outer sheath.

7. FUEL PIN SIMULATOR PROCUREMENT

A. N. Smith W. E. Baucum
R. W. McCulloch

A full-length engineering test unit of the bundle 3 fuel pin simulator design has been received from the General Electric Co. and has been analyzed at ORNL. The unit showed a good high-insulation resistance between center-line thermocouples and heating element but a somewhat low resistance between heating element and sheath. GE has indicated that the filling of boron nitride between heating element and sheath occurred over a relatively long period of time due to problems encountered in the filling, and thus it is very possible that this area contains a considerable amount of moisture which would reduce the insulation resistance. The eccentricity between heating element and sheath was generally good throughout most of its length but did exceed the specified limit in certain local areas. The maximum eccentricity of the centers was measured to be 0.038 cm (0.015 in.).

Infrared scans were made on this unit at four different orientation angles about an axis along its length. These scans showed excessive variations of up to 25% of the mean value in certain areas along the length of the unit. To determine how the observed variations correlated with variations which might be present in the heating element, a 1.22-m (4-ft) section was cut from the center of the heated length, and the heating element was removed. The heating element was subjected to infrared scanning and proved to be relatively uniform. Thus it is believed that the variations observed in the infrared scan of the fuel pin simulator are principally due to variations in BN density between the heating element and the sheath. ORNL personnel visited GE during the last week of November to discuss results of our analyses and to suggest possible improvements in their fabrication procedures.

The RAMA Corp. has fabricated a short test unit of the bundle 3 design, which should be received by ORNL during the first week of December 1977. Center boron nitride preforms have been received from Eagle Picher Industries and will be shipped to RAMA for the bundle 3 prototypes during the second week in December with the annular preforms to follow by the

first week in January 1978. RAMA should then be ready to begin fabrication of the full-length bundle 3 prototypes.

REFERENCES

1. *Quarterly Progress Report on Blowdown Heat Transfer Separate-Effects Program for April–June 1976*, ORNL/NUREG/TM-46 (January 1977).

2. *Quarterly Progress Report on Blowdown Heat Transfer Separate-Effects Program for January–March 1977*, ORNL/NUREG/TM-109 (August 1977).

3. *Quarterly Progress Report on Blowdown Heat Transfer Separate-Effects Program for April–June 1977*, ORNL/NUREG/TM-134 (November 1977).

4. L. J. Ott and R. A. Hedrick, *ORINC – A One-Dimensional Implicit Approach to the Inverse Heat Conduction Problem*, ORNL/NUREG-23 (November 1977).

5. *Quarterly Progress Report on Blowdown Heat Transfer Separate-Effects Program for July–September 1977*, ORNL/NUREG/TM-149 (in publication).

6. J. D. Sheppard, P. H. Hayes, and M. C. Wynn, "An Experimental Study of Flow Monitoring Instruments in Air-Water, Two-Phase Downflow," presented at CREST Specialists Meeting on Transient Two-Phase Flow, Toronto, Canada, Aug. 3–4, 1976 (in press).

7. O. Baker, "Simultaneous Flow of Oil and Gas," *Oil Gas J.* 53(12), 185–195 (July 26, 1954).

8. *Quarterly Progress Report on Blowdown Heat Transfer Separate-Effects Program for January–March 1977*, ORNL/NUREG/TM-109 (November 1977).

ORNL/NUREG/TM-175
Dist. Category NRC-2

Internal Distribution

1. R. K. Adams
2. J. L. Bartley
3. W. E. Baucum
4. M. Bender
5. R. E. Bohanan
6. C. Brashear
7. J. R. Buchanan
8. R. H. Chapman
9. C. J. Claffey
10. N. E. Clapp
11. V. D. Clemons
12. W. B. Cottrell
13. W. G. Craddick
14. J. L. Crowley
15. R. D. Dabbs
16. C. E. Davis
17. I. T. Dudley
18. B. G. Eads
19. G. G. Fee
20. D. E. Ferguson
21. R. M. Flanders
22. M. H. Fontana
23. U. Gat
24. M. J. Goglia
25. R. H. Greene
26. R. C. Hagar
27. J. E. Hardy
28. R. A. Hedrick
29. R. E. Helms
30. R. W. Henderson
31. H. W. Hoffman
32. J. L. Horton
33. C. R. Hyman
34. P. A. Jallouk
35. A. F. Johnson
36. T. G. Kollie
37. J. W. Krewson
38. D. M. Leon
39. Milton Levenson
40. R. E. MacPherson
41. G. S. Massengill
42. G. M. Maxwell
43. R. W. McCulloch
44. C. A. Mills
45. R. L. Moore
46. C. B. Mullins
47. F. R. Mynatt
48. F. H. Neill
49. L. J. Ott
50. H. R. Payne
51. H. Postma
52. W. Ragan, Jr.
53. J. L. Redford
54. M. J. Roberts
55. E. R. Rohrer
56. J. P. Sanders
57-58. Myrtleen Sheldon
59. R. L. Shipp
60. A. N. Smith
61. I. Spiewak
62. R. D. Stulting
63-72. D. G. Thomas
73. R. A. Todd
74. H. E. Trammell
75. D. B. Trauger
76. K. G. Turnage
77. J. L. Wantland
78. J. D. White
79. M. D. White
80. G. D. Whitman
81. L. V. Wilson
82. Patent Office
83-84. Central Research Library
85. Document Reference Section
86-90. Laboratory Records Department
91. Laboratory Records (RC)

External Distribution

92. H. R. Sebesta, Professor and Chairman, Department of Mechanical Engineering, University of Texas at Arlington, Arlington, Tex. 76019
93-100. Director, Division of Reactor Safety Research, Nuclear Regulatory Commission, Washington, D.C. 20555
101. Director, Reactor Division, DOE, ORO
102. Director, Research and Technical Support Division, DOE, ORO
103-107. Director, Reactor Safety Research Coordination Office, DOE, Washington, D.C. 20555
108-411. Given distribution as shown under category NRC-2 (25 copies — NTIS)

☆U.S. GOVERNMENT PRINTING OFFICE:1978 -740 -190/ 16